Fricción, una Propiedad Limitante en el Movimiento Controlado.

Astor García Amor

16 de agosto de 2016

Índice general

Capítulo 1

Abstracto

Este trabajo de fin de grado ha sido realizado en la Universidad de Linköping, dentro del departamento de *Ingeniería de fluidos y mecatrónica* (FLUMES), a través de un acuerdo ERASMUS entre esta y la Universidad de Oviedo.

El objetivo de este proyecto es el desarrollo de un modelo que describa el fenómeno de la fricción que se produce en los cilindros hidráulicos.

La fricción aparece como un fenómeno que reduce la eficiencia de los elementos hidráulicos y que, a su vez, obstaculiza un correcto control de estos por medio de sistemas automáticos. Por tanto, un conocimiento más profundo de esta propiedad puede permitir el diseño de sistemas de control más precisos que los actualmente existentes; algo muy interesante dada la creciente presencia de estos en la industria.

Los experimentos llevados acabo han analizado un cilindro *Bosch Reroth CGM1MF3/40/28/150A2X/B11CGDTWW*. En ellos se ha podido observar una clara dependencia entre la fuerza de fricción, la velocidad y la presión en el interior del cilindro; permitiendo el desarrollo de un modelo explicativo.

Este resultado es interesante puesto que un incremento de la carga de trabajo a la que se somete al cilindro implica un incremento de la presión interna y, por consiguiente, de la fuerza de fricción.

El modelo creado en este proyecto permitirá la implementación de sistemas de control más precisos que los actualmente existentes y que sean capaces de lidiar con diferentes condiciones de trabajo. Se trata de algo novedoso si tenemos en cuenta la escasa bibliografía que recoge el efecto de la presión sobre el comportamiento de la fricción.

Capítulo 2

Teoría

Antes de realizar cualquier tipo de experimento o cálculo conviene hacer un estudio de las teorías previas referentes al tema en cuestión. En relación con el fenómeno de la fricción, ciertos conceptos deben ser introducidos:

2.1. Fricción seca

También conocida como fricción de Coulomb. Define el fenómeno de fricción que aparece al interactuar dos superficies sin presencia de ningún fluido entre ellas.

Se caracteriza por ser directamente proporcional a la fuerza normal (F_N) entre las superficies en contacto e independiente de la velocidad relativa entre estas.

$$F_f = \mu \cdot F_N \tag{2.1}$$

2.2. Fricción viscosa

La mayoría de los contactos deslizantes están lubricados. Esto implica que la mencionada anteriormente fricción seca no describa fielmente el fenómeno.

En este caso, la fuerza de fricción se caracteriza por ser independiente (durante este proyecto se indicará que no es así) de la fuerza normal entre las superficies y proporcional a la velocidad relativa entre estas.

$$F_f = \gamma \cdot v \tag{2.2}$$

2.3. Otros efectos

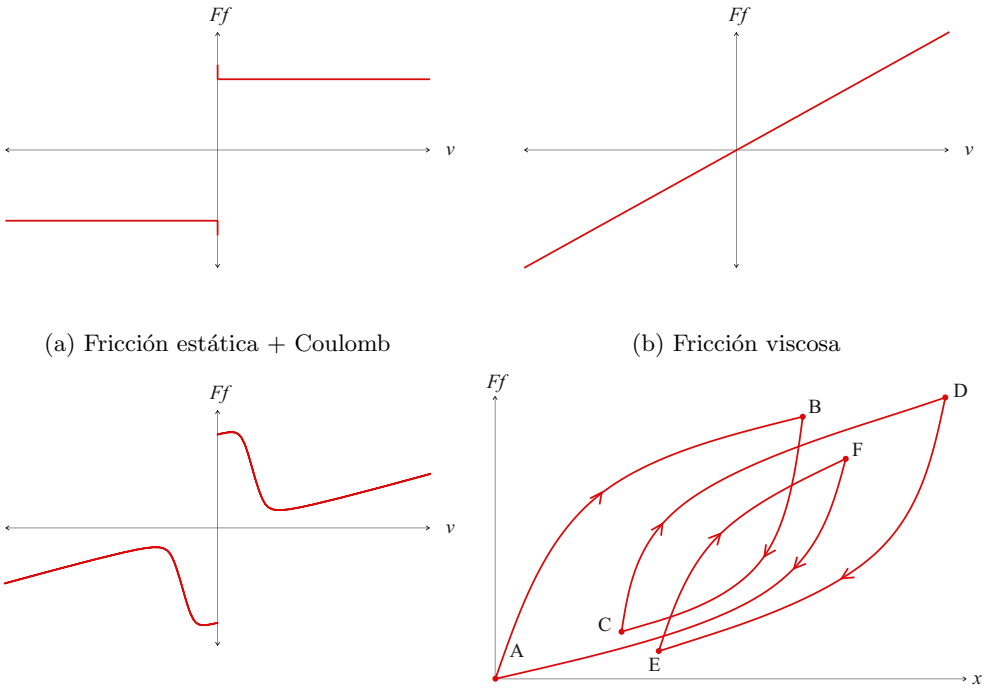

(a) Fricción estática + Coulomb

(b) Fricción viscosa

(c) Efecto Stribeck

(d) Lazos de histéresis

Figura 2.1: Fenómenos de fricción

2.3.1. Fricción estática

Cuando la velocidad relativa entre las superficies en contacto es igual a cero, la fuerza de fricción que se ha de superar para comenzar el movimiento es mayor que la correspondiente fricción dinámica.

2.3.2. Efecto Stribeck

Al analizar la fricción en contactos lubricados puede ser observado que, al principio, la fuera disminuye al aumentar la velocidad hasta que alcanza un mínimo valor. Después de este punto, la fricción comienza a aumentar comportándose tal y como indica la ley de fricción viscosa.

Este es el llamado *efecto Stribeck*. Nombrado así por Richard Stribeck, la primera persona en desarrollar un modelo capaz de explicarlo.

2.3.3. Histéresis

Este efecto muestra cómo la fuerza de fricción es dependiente de la aceleración. Así pues, con aceleraciones positivas, esta es mayor que con aceleraciones negativas.

2.4. Modelos de fricción

2.4.1. Modelo de Stribeck

Tal y como fue introducido anteriormente, el efecto Stribeck no podía ser explicado por los modelos tradicionales. Es así que él mismo desarrolló uno capaz de dar explicación a este comportamiento.

El modelo de Stribeck está basado en el cambio de las características de la frontera entre las superficies en contacto dependiendo de la velocidad.

De acuerdo con este análisis, describió 4 regímenes distintos:

- Fricción estática y comportamiento previo al deslizamiento
- Lubricación límite
- Lubricación mixta
- Lubricación (elasto) hidrodinámica

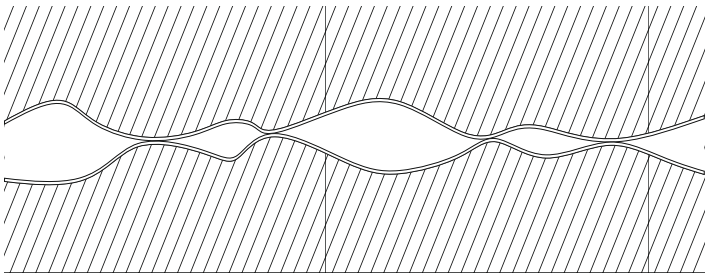

Figura 2.2: Lubricación límite

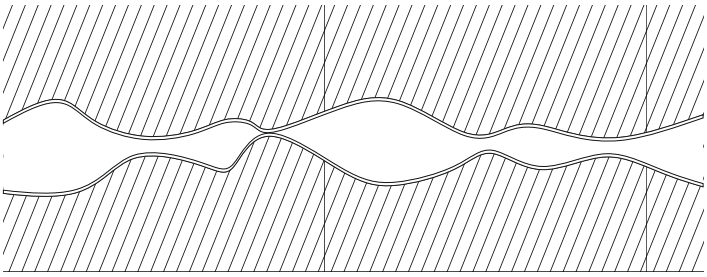

Figura 2.3: Lubricación mixta

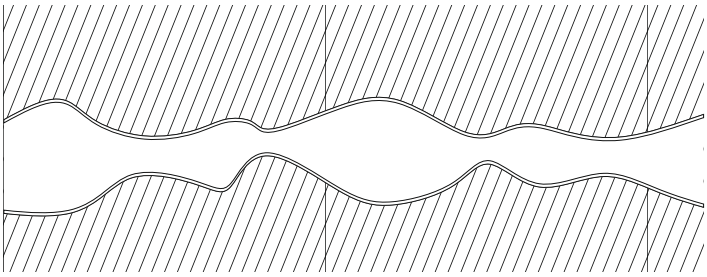

Figura 2.4: Lubricación (elasto) hidrodinámica

2.4.2. Modelo de Dahl

Este modelo supone una alternativa al modelo de Coulomb en lo que se refiere a explicar la fricción seca.

Se trata de un modelo estático que, por tanto, no considera la velocidad del deslizamiento. La fuerza de fricción se muestra como función del desplazamiento; de modo que sólo explica el comportamiento previo al deslizamiento atendiendo a la deformación de las asperezas superficiales.

2.4.3. Modelo de LuGre

Este modelo recibe su nombre por las universidades de Lund y Grenoble con cuya colaboración pudo ser desarrollado. Añade la fricción viscosa y el efecto de Stribeck al modelo de Dahl. Es, por tanto, un modelo dinámico que además considera, no sólo la velocidad, sino también la aceleración.

Una característica importante es que, con velocidades constantes (sin aceleración), la curva de fricción termina comportándose tal y como el modelo de Coulomb predice.

El modelo de LuGre puede ser expresado de acuerdo a las siguientes ecuaciones

$$\begin{aligned} F &= \sigma_0\, z + \sigma_1\, \dot{z} + f(v) \\ \frac{dz}{dt} &= v - \sigma_0\, \frac{|v|}{g(v)}\, z = v - h(v)\, z \\ g(v) &= F_c + (F_s - F_c)\, e^{-\left(\frac{v}{v_r}\right)^{\alpha}} \end{aligned} \tag{2.3}$$

Donde:

σ_0	dureza para un comportamiento elástico a pequeños desplazamientos
z	estado interno de fricción
$g(v)$	función dependiente de la velocidad
σ_1	amortiguamiento adicional asociado con micro-desplazamientos → fricción viscosa
$f(v)$	término dependiente de la velocidad. Para fricción viscosa, normalmente $f(v) = \sigma_2\, v$
F_s	fricción estática
F_C	fuerza de Coulomb
v_r	parámetro que determina la velocidad con la que $g(v)$ se aproxima a F_c, normalmente simplificado como v_s
α	valores normales comprendidos entre 0.5 y 2

En el caso de *velocidad constante* (steady state), la fuerza de fricción puede ser expresada como:

$$F_{ss} = g(v_{(t)}) + f(v) \tag{2.4}$$

Que, desarrollada puede ser escrita como:

$$F_{ss} = F_c + (F_s - F_c)e^{-\left(\frac{v}{v_r}\right)^{\alpha}} + f(v) \tag{2.5}$$

2.4.4. Modelo dependiente de la presión

Los modelos anteriores consideraban la fricción como dependiente de la velocidad o, en el caso del modelo de Dahl, del desplazamiento. Sin embargo, cualquier experimento que se lleve a cabo con cilindros hidráulicos muestra que la presión tiene un efecto muy significativo en la fricción. Esto puede ser explicado analizando el comportamiento de las juntas. Estas son afectadas por la presión en el interior de las cámaras del cilindro y modifican su ajuste contra las paredes del cilindro y del pistón. Ello implica un aumento de las fuerzas normales y, como consecuencia, de la fricción, tal y como sugiere la primera ley de la fricción.

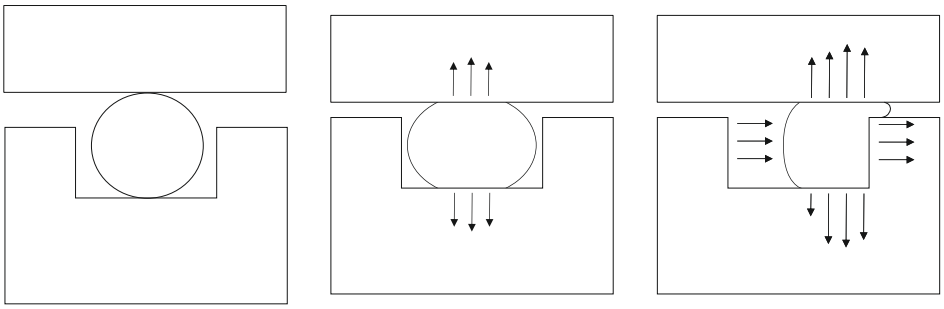

Figura 2.5: Comportamiento de una junta de tipo O-Ring cuando se le aplica presión

2.4.5. Modelo completo

Tras estudiar los diferentes modelos, es posible desarrollar uno propio que recoja las diferentes características consideradas anteriormente.

Pese a que existen modelos más sofisticados que los analizados anteriormente, el modelo de LuGre parece ser un buen punto de partida. Dada la conocida influencia de la presión en el comportamiento de la fricción, se intentará desarrollar esta dependencia.

Capítulo 3

Trabajo experimental

En los capítulos anteriores se realizó un estudio de la naturaleza de la fricción y se introdujeron diversas teorías explicativas. El siguiente paso es llevar acabo los experimentos necesarios para analizar el comportamiento de nuestro cilindro y ser capaces de introducir un modelo válido.

Para el experimento, se ha analizado la respuesta a diferentes presiones de un cilindro hidráulico simétrico proporcionado por *Bosch Rexroth* en un banco hidráulico típico para ensayos de resistencia de materiales. El esquema puede ser visto en la siguiente figura.

Para poder realizar este experimento, ha sido necesario el diseño y construcción de una estructura de soporte así como un adaptador para conectar el pistón del cilindro con la célula de carga que aporta los datos experimentales.

El montaje consiste en: el cilindro (1), la prensa hidráulica (2), la estructura de soporte (3), una célula de carga (4) y una bomba hidráulica manual (5)

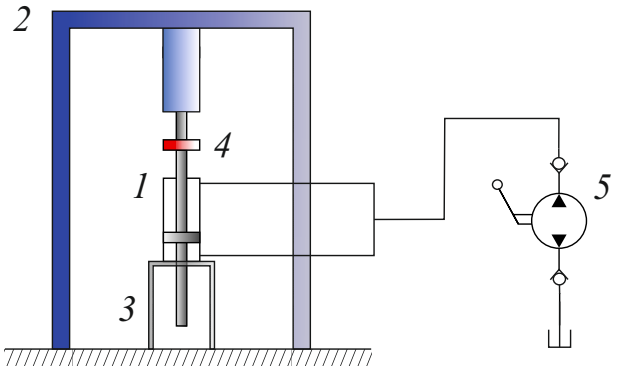

Figura 3.1: Montaje experimental

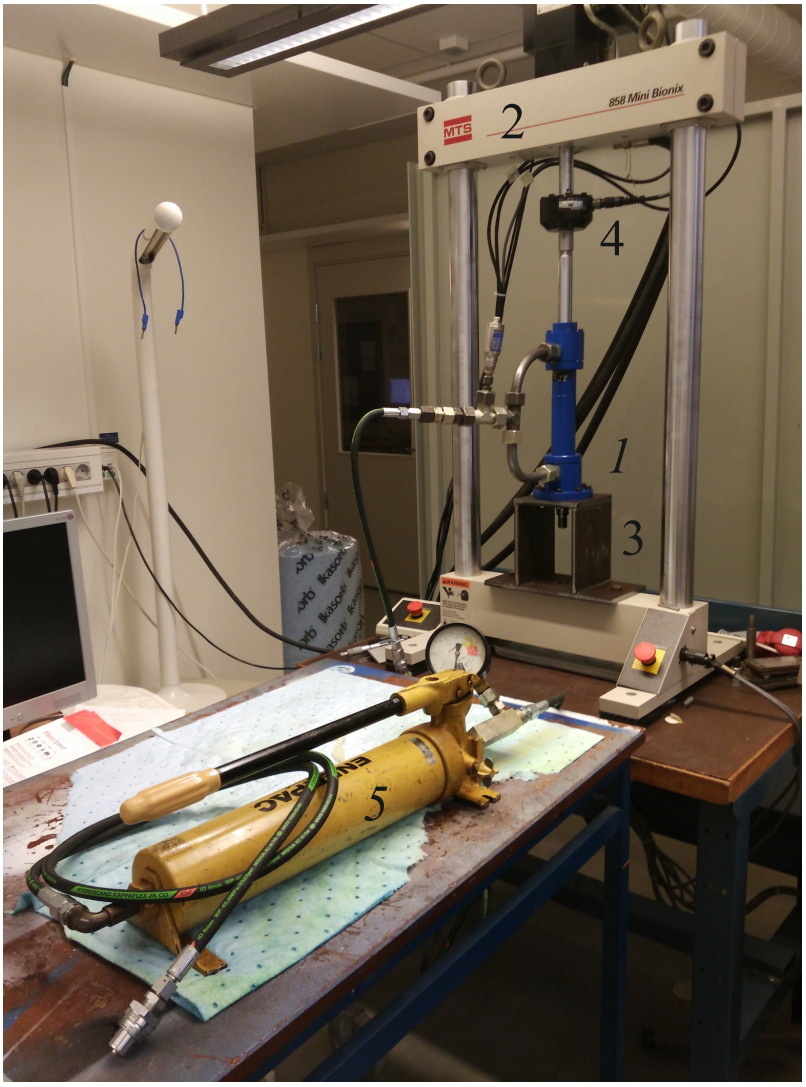

Figura 3.2: Montaje experimental en el laboratorio con bomba manual

Capítulo 4

Resultados

Tras analizar los datos obtenidos en el experimento, se ha podido desarrollar una variación del modelo de LuGre que tiene en cuenta el efecto de la presión en la fricción.

$$F_f = F_c + (F_s - F_c)e^{-\left(\frac{v}{v_r}\right)^{\alpha}} + \sigma_2\, v \qquad \text{(2.5 rev)}$$

La dependencia de la presión de los parámetros Fs, Fc, and σ_2 puede ser descrita de forma precisa tras analizar los resultados experimentales, tal y como se puede observar en las siguientes fórmulas:

$$F_c = F_c(p) = 70,2 + 0,5\, p \tag{4.1}$$

$$F_s = F_s(p) = 112{,}9 + 0,6\, p \tag{4.2}$$

$$\sigma_2 = \sigma_2(p) = 0{,}34 + 8 \cdot 10^{-4}\, p \tag{4.3}$$

Donde F_c y F_s son dados en N, σ_2 es dado en $\mathrm{N\,s\,mm^{-1}}$ y p en bar.

Por otro lado, α, v_r, y la velocidad de Stribeck (v_s) no parecen reflejar ningún tipo de relación con la presión. Es más, la gran variabilidad de estos parámetros hace difícil escoger un valor adecuado, únicamente permitiendo la elección de un rango aproximado.

Tras realizar diferentes simulaciones con valores cambiantes de estos parámetros, se puede concluir que un valor de $\alpha = 1$ y $v_r = 10\,\mathrm{mm\,s^{-1}}$ proporciona un modelo simple y preciso.

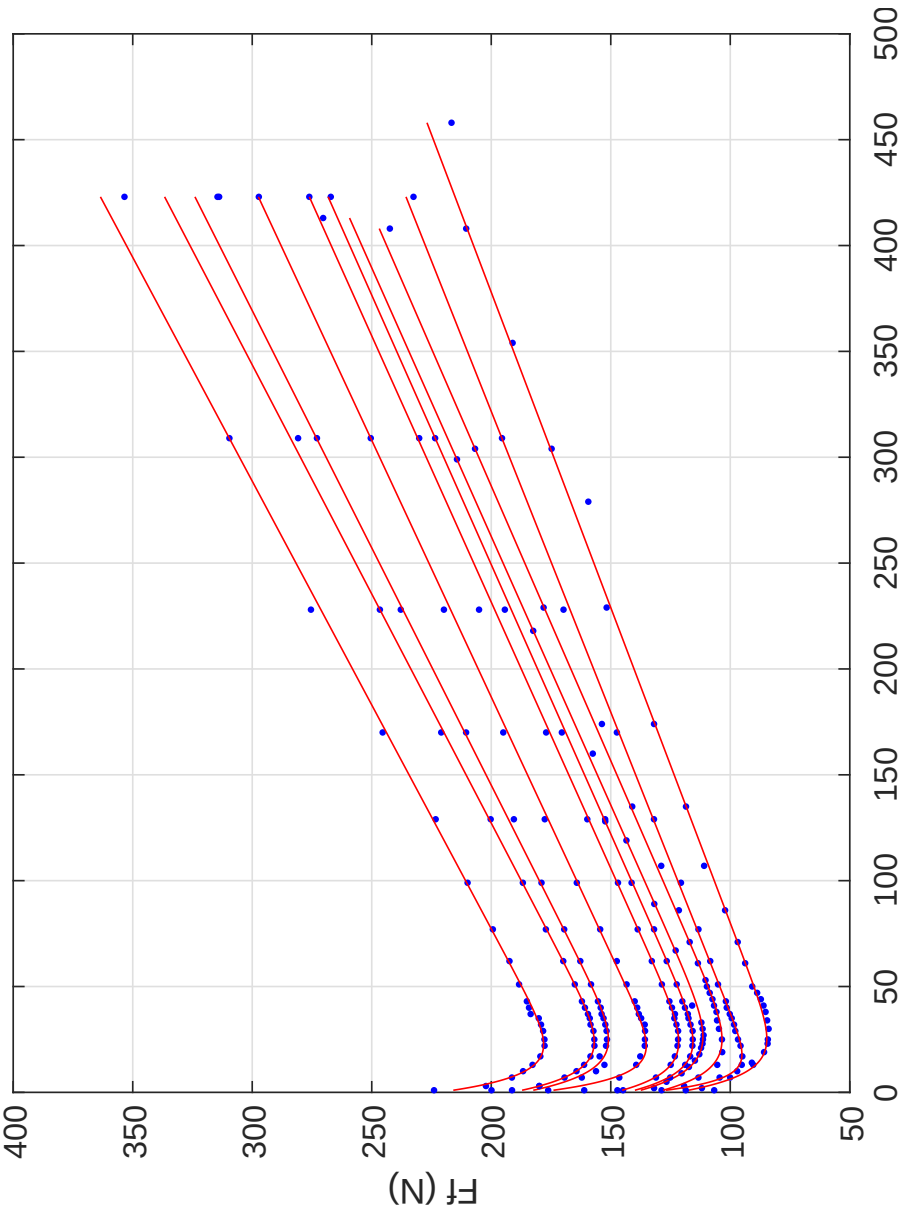

Figura 4.1: Ajuste experimental de datos. Presiones equidistantes desde 0.1 a 159 bar

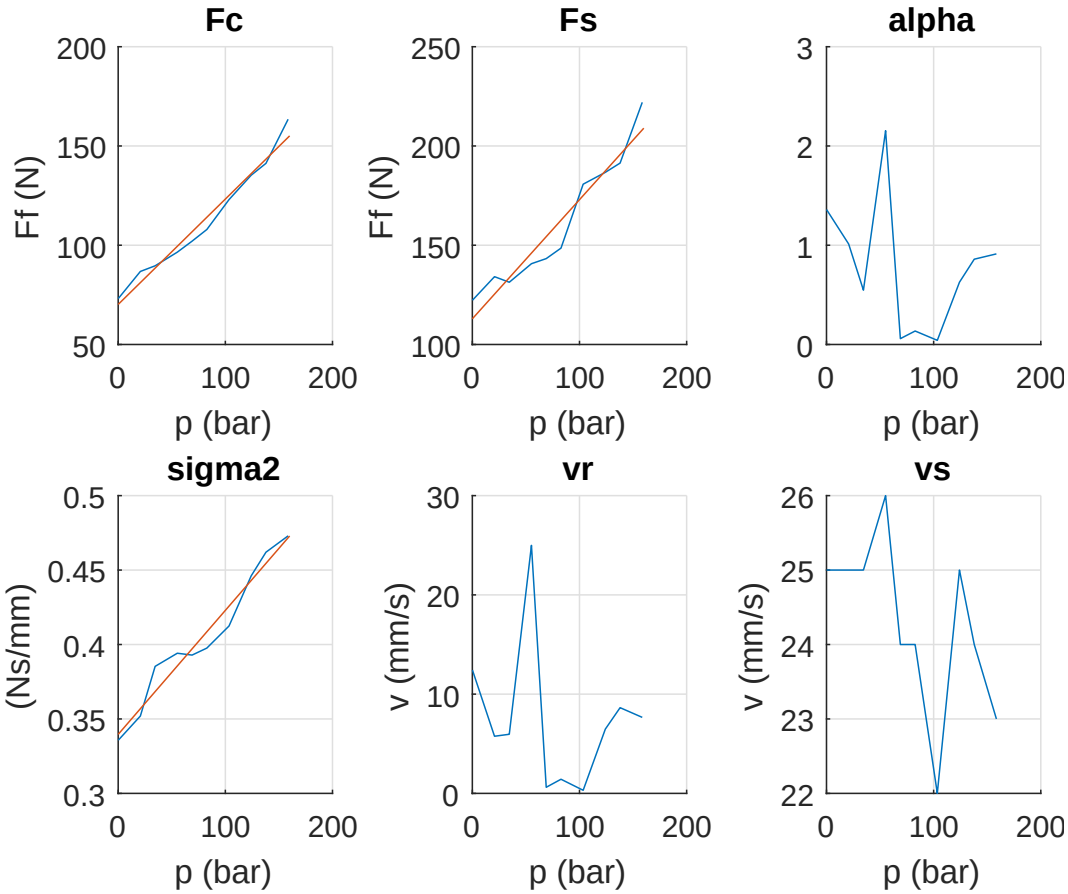

Figura 4.2: Variación de los parámetros con la presión

Capítulo 5

Conclusión

Los resultados obtenidos muestran cómo la fuerza de fricción está altamente influenciada por la velocidad y la presión dentro del cilindro. Mientras que la primera es un factor cuya influencia está contemplada en diferentes modelos, la presión suele ser olvidada pese a haber demostrado afectar de forma importante a este fenómeno.

La creación de un modelo descriptivo del fenómeno de fricción busca poder ser extendido a cualquier cilindro con el que se trabaje. Conocidos unos factores propios en cada caso, deberían poder ajustarse las ecuaciones que definen los diferentes parámetros.

Puesto que la influencia de la presión procede del comportamiento de las juntas y la variedad de estas es limitada para cada fabricante, puede ser interesante sugerir el desarrollo de experimentos propios para indicar los factores determinantes de cada junta en el catálogo y permitir una elección adecuada, atendiendo a los requerimientos, del producto por parte de los clientes.

LINKÖPING UNIVERSITY

Friction, a Limiting Property in Controlled Motion

Astor
Garcia Amor

Division of Fluid and Mechatronic Systems

Bachelor Thesis
Department of Management and Engineering
LIU-IEI-TEK-G- -16/01080- -SE

Friction, a Limiting Property in Controlled Motion

Bachelor Thesis in Fluid Power
Department of Management and Engineering
Division of Fluid and Mechatronic Systems
Linköping University
by

Astor
Garcia Amor

LIU-IEI-TEK-G- -16/01080- -SE

Supervisors: **Martin Hochwallner**
IEI, Linköping University

Examiner: **Liselott Ericson**
IEI, Linköping University

Linköping, 6 June, 2016

Upphovsrätt

Detta dokument hålls tillgängligt på Internet — eller dess framtida ersättare — under 25 år från publiceringsdatum under förutsättning att inga extraordinära omständigheter uppstår.

Tillgång till dokumentet innebär tillstånd för var och en att läsa, ladda ner, skriva ut enstaka kopior för enskilt bruk och att använda det oförändrat för ickekommersiell forskning och för undervisning. Överföring av upphovsrätten vid en senare tidpunkt kan inte upphäva detta tillstånd. All annan användning av dokumentet kräver upphovsmannens medgivande. För att garantera äktheten, säkerheten och tillgängligheten finns det lösningar av teknisk och administrativ art.

Upphovsmannens ideella rätt innefattar rätt att bli nämnd som upphovsman i den omfattning som god sed kräver vid användning av dokumentet på ovan beskrivna sätt samt skydd mot att dokumentet ändras eller presenteras i sådan form eller i sådant sammanhang som är kränkande för upphovsmannens litterära eller konstnärliga anseende eller egenart.

För ytterligare information om Linköping University Electronic Press se förlagets hemsida `http://www.ep.liu.se/`

Copyright

The publishers will keep this document online on the Internet — or its possible replacement — for a period of 25 years from the date of publication barring exceptional circumstances.

The online availability of the document implies a permanent permission for anyone to read, to download, to print out single copies for his/her own use and to use it unchanged for any non-commercial research and educational purpose. Subsequent transfers of copyright cannot revoke this permission. All other uses of the document are conditional on the consent of the copyright owner. The publisher has taken technical and administrative measures to assure authenticity, security and accessibility.

According to intellectual property law the author has the right to be mentioned when his/her work is accessed as described above and to be protected against infringement.

For additional information about the Linköping University Electronic Press and its procedures for publication and for assurance of document integrity, please refer to its www home page: `http://www.ep.liu.se/`

© Astor
Garcia Amor

Abstract

The aim of this thesis is the development of a model to describe the friction phenomena in hydraulic cylinders.

Friction appears as a phenomena that reduces the efficiency of hydraulic elements but also that obstacles a proper control by automatic systems. A further understanding of this property may allow to design better and more accurate control systems, which are becoming more frequent each day.

By experimenting with a symmetric hydraulic cylinder *Bosch Rexroth* CGM1MF3/40/28/150A2X/B11CGDTWW, a clear dependence of the friction force from the pressure has been displayed and a model to gather the results has been created.

An increase of the load under which a cylinder works implies a rise of the friction force. Such effect is modelled at the end of this project. This will be useful in order to implement new control systems to deal with variable working conditions. Something innovative, taking into account the lack of literature considering the effect of pressure on the behaviour of friction.

Acknowledgments

This thesis has been performed at Linköping University within the area of Fluid and Mechatronic Systems *Flumes*. This work could not have been possible without the collaboration of different people to who I am really grateful.

I would like to express my gratitude to my supervisor Martin Hochwallner. His enthusiasm and support encouraged me to carry out this project although all the challenges and difficulties I had to face.

Liselott Ericson, who gave me the possibility of performing the thesis within fluid mechanics and provided me with really important knowledge through the course *Fluid Power Systems* that I could take here in Linköping University. As well, this work would not have been possible without her approachability and help, that allowed me to solve immediatly any issue.

Particular thanks goes to Patrik Harnman, who spent his time helping me with the experiment.

Special thanks go to *Bosch Rexroth* for providing two cylinders and make the experiment possible.

I want to thank my family, that supported me and brought me the opportunity to come to Linköping University and, especially, to my brother Illán who, apart from introducing me to LaTeX, has always been there to give me the help I needed.

Before finishing this acknowledgements, I cannot forget about friends: the old ones, that have always been there although my difficulties to keep in touch; the new ones, which I am sure will be part of the old ones one day; and those who, although the distance and the cold, came to give me the energy I needed.

Linköping, June, 2016

Astor
García Amor

Contents

List of Figures

List of Tables

Chapter 1

Introduction

In a world where fluid power systems are becoming more and more popular due to its high power density and the variety of possibilities that they offer, improving their efficiency and understanding their behaviour becomes crucial.

As well as in the majority of constructions, friction appears as a phenomena which determines their performance. That is a major reason why its study has such great interest.

The increasingly use of automatic systems in nowadays applications requires from a deep understanding of the characteristics of this phenomena in order to achieve a more accurate control. Although there are several friction models that try to explain it, conventional software considers a simple approach of the real response of the systems. In addition, the influence of the load conditions is barely taken into account.

1.1 Aims

The aim of this thesis, is to determine a precise model of friction and study the influence of the load under which the system works. The object of study is a symmetric cylinder *Bosch Rexroth* CGM1MF3/40/28/150A2X/B11CGDTWW provided by Bosch Rexroth. However, the overall results can be applied to any hydraulic cylinder of similar characteristics.

1.2 Research question

In order to set and delimit the scope of this project, the research question must be considered:

What is friction and what are the main factors that affect it? Is it possible to predict the behaviour of the friction forces in a cylinder from its data sheet?

1.3 Ethics

When accomplishing any project, the ethic aspects have to be always in mind. It is a fact that certain subjects are more prone to have ethical dilemmas, however a quick analysis can be interesting in any project.

The environmental impact is a subject that concerns to everyone. The conditions under which the experiments where performed implied the use of mineral oil, known to be harmful for the environment. Nevertheless, taking care with the handling and performing a responsible disposal of the waste can minimize this effect.

Another aspect that could be considered is the use of the results of this thesis with bad purposes. Although technology should be employed to help humanity, sometimes it becomes one of the most harmful weapons. Due to the scope and transcendence of this project, this subject is far from being disturbing.

Chapter 2

Friction

Talk about friction implies a reference to *tribology* and its history. A deeper look at the article "Industrial Tribology: Tribosystems, Friction, Wear and Surface Engineering, Lubrication" [7] can provide interesting information about the subject. The field of tribology is related to the study and application of friction, lubrication and wear. This term comes from the Greek *tribos*, which means *rubbing*, but it was not until 1966 when it was first used in the *Jost Report*. This was a study carried out by the Government of the United Kingdom with the purpose of determining the cost that loses due to friction were causing to the country.

Friction appears as a force against movement. It is usually considered as something harmful, since we associate it to a higher energy consumption (for example cars, bicycles, motors...). But it also provides support to basic activities as walking, grabbing a cup or even standing up.

Attempts of avoiding the unwanted friction effects have been recorded since the earliest times. An egyptian painting from the tomb of Tehuty-Hetep shows an man pouring lubricant in front of a sledge on which a sculpture was being transported.

Not surprisingly, Leonardo da Vinci did really important research about the friction phenomena back in the 16th century, setting two main principles that would serve as the basis for the understanding of friction. These were the **proportionality of the friction force with the applied load** and the **independence of the apparent area of contact**.

However, it was Guillane Amontons in December 1699 who presented the details of his experimental results and setted these results as the **first and second laws of friction**.

With the Industrial Revolution and the rapid technological development, the improvement of bearings and the reduction of friction was a priority. As well as the technological development, the scientific discoveries were also boosted in those days. Considering the contribution to the tribology field, a name must be mentioned: Charles Augustin Coulomb. He explained the behaviour of dry contacts in a way that is still used nowadays. Regarding lubrication and other different areas related with fluid dynamics, scientists such as Leonhard Euler,

Daniel Bernoulli, Claude Navier, showed up with researches that contributed to a better definition of the viscous friction.

Few years later, at the beginning of the 19th century, Richard Stribek developed one of the most complete and accurate models describing the friction phenomena in lubricated sealing by introducing the called: *Stribeck effect*. In this effect is in which this thesis has its main focus.

Before starting with the experimental approach, any project requires from a previous study of former theories in order to use the knowledge they provide. As Isaac Newton said:

'If I have seen further, it is because of standing upon the shoulders of giants'

For this project, a review of the friction phenomena and models existing will provide an appropriate starting point.

2.1 Friction phenomena

The friction effect has been studied from a long time, bringing about different theories which tried to explain it in a better or worse way. Nowadays, a deep knowledge about it has been achieved and recorded.

Some extra read at the thesis "Friction Models and Friction Compensation" (p6) [4] and the work "Fundamentals Of Friction Modelling" [2] can add useful information to this topic.

2.1.1 Dry friction

The first consideration about friction that will be explained, due to its simplicity but also applicability for most of the cases is the *Coulomb friction*, named after Charles-Augustin de Coulomb. It is the first approximation to the dry friction. It states a model based in the three laws of dry friction:

- **Amonton's First Law**: the force of friction is directly proportional to the normal force between the surfaces.
- **Amonton's Second Law**: the force of friction is independent of the contact area.
- **Coulomb's Law of Friction**: the force of friction is independent of the relative velocity of the surfaces.

Coulomb friction can be modelled as it follows:

$$F_f = \mu \cdot F_N \tag{2.1}$$

2.1.2 Viscous friction

Most of the sealing that are designed to slide are lubricated. This makes the previous *dry friction* not applicable, consequence of a completely different behaviour characterised by the proportionality to the relative velocity between the surfaces, which is stated according to the next law:

$$F_f = \gamma \cdot v \tag{2.2}$$

This phenomena is shown in the figure 2.1b.

2.1.3 Other effects

Although the main friction phenomena follows the previous laws, some effects cannot be explained without other theories.

Stiction

A phenomena that can be observed at figure 2.1a is the stiction, which comes from static friction. This force appears when the relative velocity between the surfaces is equal to zero and characterizes for being higher than the dynamic friction force.

This effect can be modelled the following way:

$$F_f = \begin{cases} F_e & \text{if } v = 0 \text{ and } |F_e| < F_s \\ F_s \operatorname{sgn}(F_e) & \text{if } v = 0 \text{ and } |F_e| \geq F_s \end{cases} \tag{2.3}$$

Where:

F_e external force applied

F_s stiction force

Stiction brings about a behaviour called **stick-slip**, characterized by a discontinuous jerking motion that appears at low velocities.

Stribeck effect

When analysing the friction in lubricated sealing at constant velocity values, it can be observed that, at the beginning, the force decreases for increasing velocities until it reaches a minimum value at the the *velocity weakening*, as it can be seen at figure 2.1c, after which it really starts behaving as expected according to the viscous friction law. This is the called *Stribeck effect*, named after Richard Stribeck, who was the first person in developing a model to explain it.

Although not that clearly, the same effect can be observed in dry friction.

Friction Lag

Another effect that cannot be explained using the previously explained laws is the *friction lag*, also called *friction hysteresis* (see figure 2.1d).

Former experiments had been developed at constant velocities; however, when doing them at changing velocities, the behaviour differs, as friction force is higher for increasing (acceleration) than for decreasing velocities (deceleration).

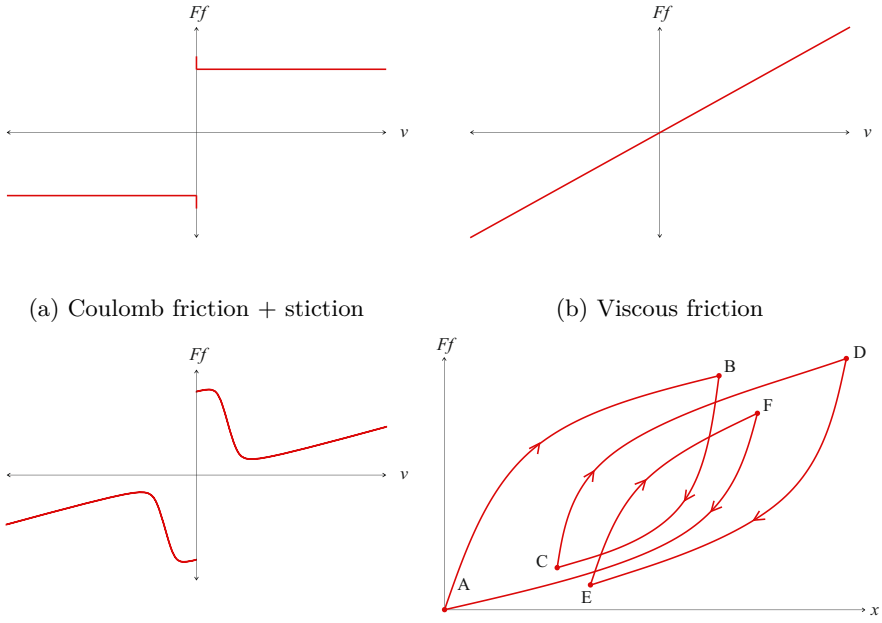

(a) Coulomb friction + stiction

(b) Viscous friction

(c) Stribeck effect

(d) Hysteresis loops

Figure 2.1: Friction phenomena

2.2 Friction models

In order to explain the friction phenomena, several models have been developed along the time. From the first *static models* which showed up not to be enough to give a complete explanation for the characteristics of the friction phenomena, to the more complete and detailed, but also complex *dynamic models*.

2.2.1 Stribeck model

As it was introduced before, the Stribeck effect could not be explained by the traditional friction models. However, he himself developed one, providing an explanation to this behaviour.

Stribeck's model is based on the changing boundary between the surfaces in contact depending on the velocity. According to this, four dynamic regimes are introduced.

Static friction and presliding displacement

In this regimen, at zero velocity, the contact appears at asperity junctions. The friction forces at this point are due to the elastic deformation of this asperity junctions and to the plastic deformation of both: the boundary film and the junctions.

Boundary lubrication

This regimen appears at low velocity. In this situation, the velocity cannot build a fluid film of lubricant between the surfaces and, as a consequence, the friction phenomena is mainly of dry nature (see 2.2).

Due to the shear between the solids, the friction during this regimen is considered to be higher than in the following ones. However, this does not always occur. As a consequence, the characteristic segment related to this regimen that is placed in the curve between the static friction and the beginning of the partial fluid lubrication (see 2.5) can be neglected in some cases.

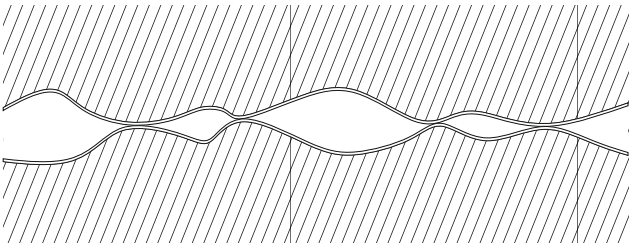

Figure 2.2: Boundary lubrication

Partial fluid lubrication

At this regimen, the velocity is enough to develop a thick lubricant layer over nearly all the surface but in some asperities. This makes the contact being mainly viscous (see figure 2.3).

Full fluid lubrication

This regimen is characterised for the absence of contact between the two surfaces (see 2.4). The whole contact is done with the lubricant layer between them and, consequently, the behaviour totally responds to the viscous friction law.

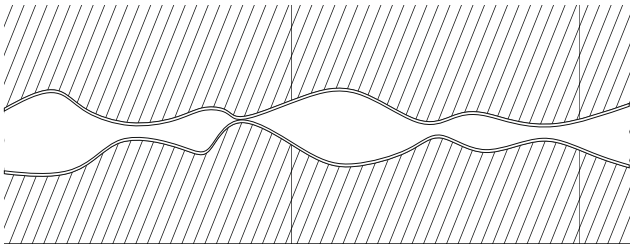

Figure 2.3: Partial fluid lubrication

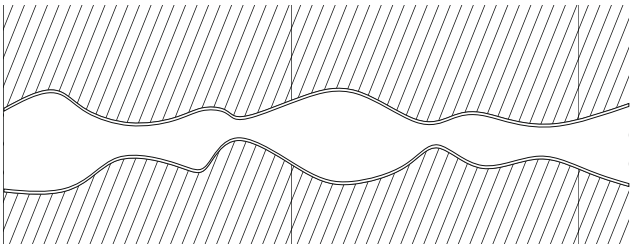

Figure 2.4: Full fluid lubrication

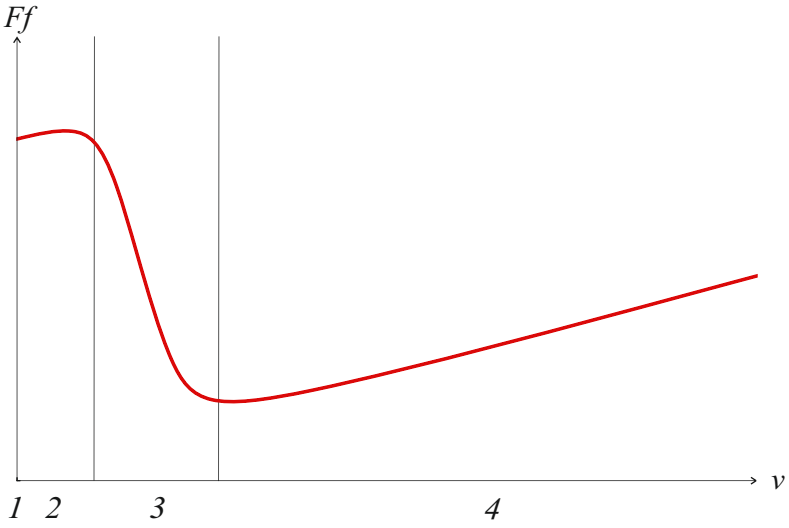

Figure 2.5: Stribeck regimes

1 Static friction and presliding displacement

2 Boundary lubrication

3 Partial fluid lubrication

4 Full fluid lubrication

2.2.2 Dahl model

The Dahl model provides an alternative to Coulomb friction model when explaining dry friction phenomena. As Coulomb's, it is a static model that does not take into account the velocity of the sliding. This model characterises for comparing the friction phenomena with the stress-strain behaviour, setting **friction as a function of displacement**. However, it only relates to pre sliding regime.

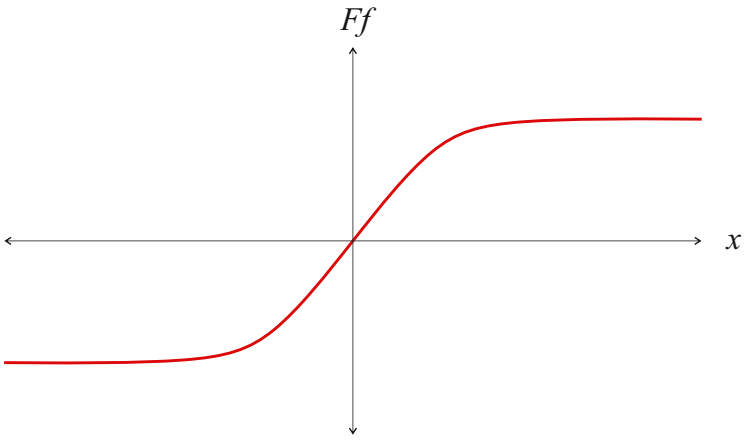

Figure 2.6: Dahl model

The *bristle model* analogy (see 2.7) is frequently used to show the behaviour at this regime:

- At the beginning, with small displacement, the bristle deforms elastically, with the possibility to return back to the original position.

- Once the elastic limit is overpassed, the bristle continues deforming plastically, bringing about non-linearities.

Dahl model is defined through the following equation:

$$\frac{dF_f(x)}{dx} = \sigma \left(1 - \frac{F_f}{F_c} \operatorname{sgn}(v)\right)^i \tag{2.4}$$

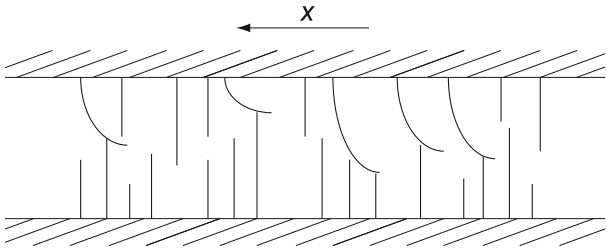

Figure 2.7: Bristle analogy

Where:

σ slope of the force-deflection curve.

i order of the slope $\begin{cases} 0 \leq i \leq 1 & \text{brittle materials (fragiles)} \\ i \geq 1 & \text{ductile materials} \end{cases}$

F_c sliding Coulomb friction: $F_N \cdot \mu = \text{constant}$

From equation (2.4), two things can be observed:

- As F_f approaches to F_c, it evolves more smothly.
- After $F_f = F_c$, the friction force keeps constant.

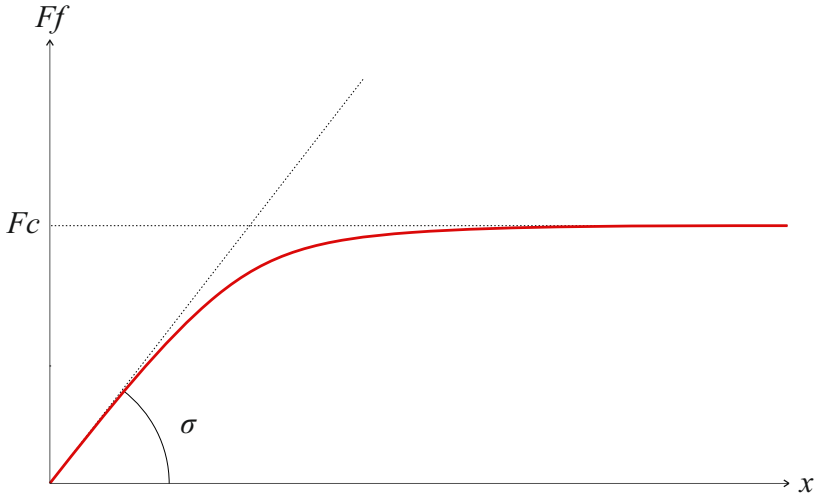

Figure 2.8: Dahl behaviour

A further explanation can be found at the thesis "Dahl Friction Modeling" [9] carried at the MIT.

2.2.3 LuGre model

The LuGre model, named after the universities of Lund and Grenoble, goes a step further. It adds the viscous friction and the Stribeck effect to the Dahl model. In addition, it is a *dynamic* model, which means that considers not only the velocity, but also the acceleration. Another characteristic is that, at steady state, the friction curve eventually behaves as the Coulomb model predicts.

LuGre model can be expressed according to the next equations.

$$\begin{aligned} F &= \sigma_0\, z + \sigma_1\, \dot{z} + f(v) \\ \frac{dz}{dt} &= v - \sigma_0\, \frac{|v|}{g(v)}\, z = v - h(v)\, z \\ g(v) &= F_c + (F_s - F_c)\, e^{-\left(\frac{v}{v_r}\right)^{\alpha}} \end{aligned} \tag{2.5}$$

Where:

σ_0	stiffness for a spring-like behaviour for small displacements
z	internal friction state
$g(v)$	velocity dependent function
σ_1	additional damping associated with micro-displacement $\rightarrow$ viscous friction
$f(v)$	memoryless velocity dependent term. For viscous friction, normally $f(v) = \sigma_2\, v$
F_s	stiction force
F_C	Coulomb force
v_r	parameter that determines how quickly does $g(v)$ approach to F_c, normally simplified as v_s
α	normal values between 0.5 and 2

In the case of *steady state*, the friction force can be expressed as it follows:

$$F_{ss} = g(v_{(t)}) + f(v) \tag{2.6}$$

Which extended is written as:

$$F_{ss} = F_c + (F_s - F_c) e^{-\left(\frac{v}{v_r}\right)^{\alpha}} + f(v) \tag{2.7}$$

The figure 2.9 shows how the curved predicted by the LuGre model can be obtained as the sum of the curve $g(v)$, which represents the Stribeck effect, and the $f(v)$ slope, that defines the viscous friction.

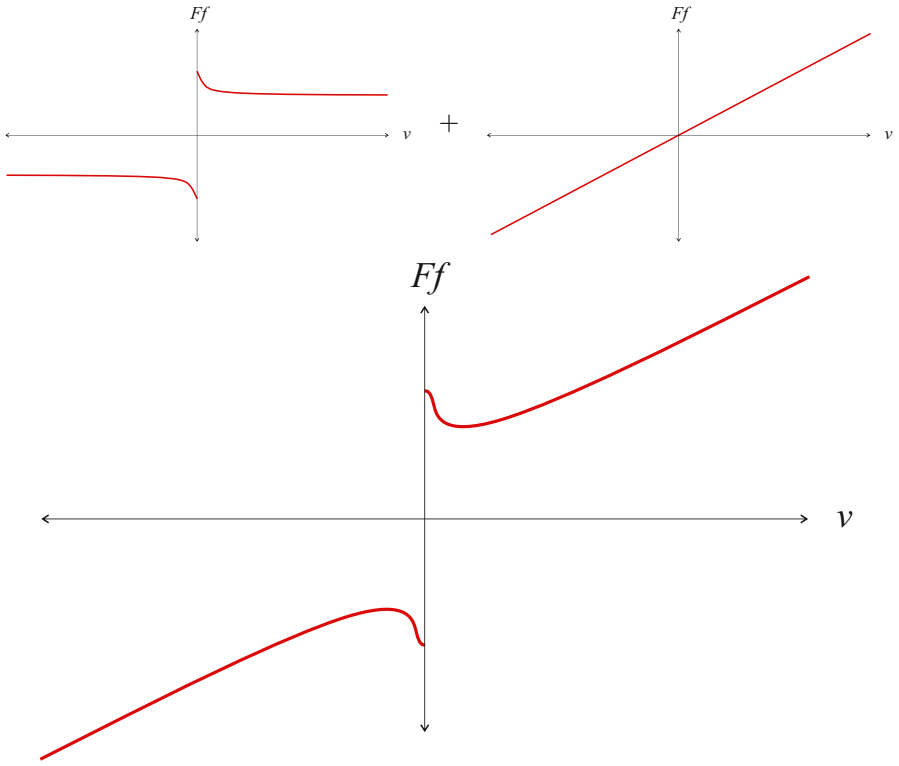

Figure 2.9: LuGre components

For further knowledge, a review at the thesis "Revisiting the LuGre friction model" [5] can be interesting.

2.2.4 Pressure dependence model

The previous models consider friction as dependent on velocity or, as it shows Dahl model, displacement. However, any experiment carried out with hydraulic cylinders shows that pressure has a significant effect on friction. This can be explained analysing the behaviour of the seals. These seals are affected by the pressure inside the chambers and change their tightness to the rod and the walls of the cylinder. This increases the normal forces and, consequently, the friction force as the **1st friction law** suggests.

Despite the transcendence of this model, few literature examines it as deep as it deserves. This is one of the reasons that has motivated this thesis.

In the following **summary model**, some assumptions about this pressure dependence are made as it is shown in the figures 2.10 and 2.11.

2.3 Summary model

After reviewing different models and having studied the friction phenomena, it is possible to make an own model which gathers the different characteristics described in the the ones mentioned before. As well, further research will provide some knowledge to approach this task with the maximum rigour.

Although more sophisticated models exist, due to the nature of this project, LuGre model seems to be a good starting point as it provides a more than enough accurate approach of the friction force by considering the Stribeck effect as well as the stiction force, and all that without becoming too complicated. However, pressure dependence is not consider and, hence, some modifications must be made.

Further tribology studies show how the Stribeck curve, in which previously friction force was introduced as velocity dependent, does actually depend on the called *Hersey number*, a dimensionless number characterized by:

$$Hersey\ number = \frac{Velocity\ (m/s) \cdot Dynamic\ viscosity\ (Pa \cdot s)}{Load\ per\ unit\ of\ lenght\ of\ bearing\ (N/m)} \tag{2.8}$$

The Hersey number shows how the regimen between two sliding surfaces evolve depending on several factors and how this affect the *friction coefficient*.

From this approach, the friction coefficient (see 2.10 and 2.11) is used as proportional to the friction force, as a remaining of the commonly employed model of dry friction.

For a better understanding, have a look at the article "Generating a Stribeck Curve in a Reciprocating Test" [8].

Influence of pressure - Hersey number

Before, it was introduced the concept of *Hersey number* and its effect on friction. According to this theory, pressure is defined as the load applied to the contact divided by the area. Consequently, if the pressure of the chambers wants to be considered, further assumptions and modifications must be made.

If, in a first approach for our system, the load over the seals of the cylinder is considered proportional to the load applied to the cylinder, the figures 2.10 and 2.11 could give a sight of how the behaviour of the friction would be under different load conditions.

This behaviour can be explained considering the friction regimes between the contact. An increase on the pressure will necessary delay the transition by obstructing the apparition of the lubricant layer between the junction.

Here, another consideration must be made: the variation of viscosity due to pressure.

According to several authors (see *Tribology* [11]) the increase of viscosity with pressure of the lubricant is considered to be nearly exponential. This relationship can be expressed with the Barus equation for isothermal viscosity pressure dependence:

$$\mu = \mu_0 \cdot e^{\alpha p} \tag{2.9}$$

Where:

μ_0	absolute viscosity at $p = 0$	$\mathrm{N\,s\,m^{-2}}$
α	pressure viscosity coefficient	$\mathrm{m^2\,N^{-1}}$
p	pressure	Pa

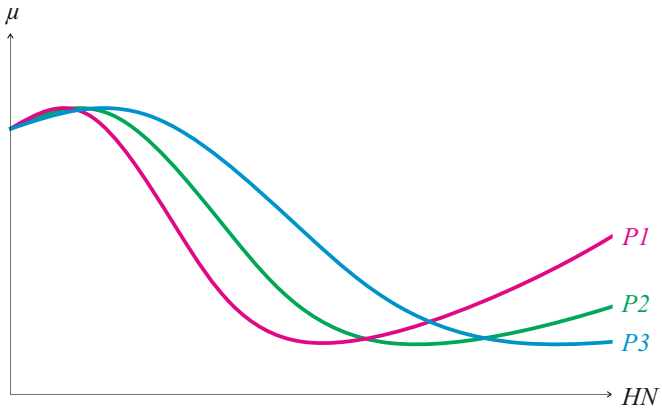

Figure 2.10: Influence of pressure. v_s affected

However, despite this exponential relationship, due to the common values of α that commercial lubricants take (between 18×10^{-9} and $28 \times 10^{-9}\,\mathrm{m^2\,N^{-1}}$, this variation can be considered negligible.

As well, another consideration can be introduced into this theoretical model: the variation of *Static friction* due to the pressure.

Stiction, introduced in 2.1.3, refers to the force that appear against the beginning of the movement. According to the theory, at this moment, there is no lubricant between the surfaces and, consequently, the contact can be defined as "dry". Taking this into account, and remembering the first dry friction law:

> *The force of friction is directly proportional to the normal force between the surfaces*

It can be deduced that the static friction will increase with the pressure.

If no other parameter change and, considering that in the full fluid lubrication regimen, friction does not depend on the pressure (the viscosity change can be neglected), the variation of friction with pressure can be expected as it is shown in the figure 2.11.

Sealing geometry

When studying the friction in a cylinder, a question may arise: where does actually appear the friction? This has an easy answer: at the seals. Consequently, the

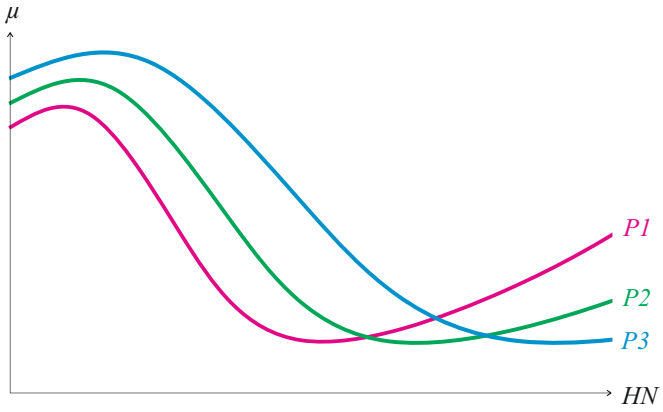

Figure 2.11: Influence of pressure. Stiction and v_s affected

geometry, material and other characteristics of these are worth studying as some important information can be extracted from them.

The cylinder of this study presents two types of seals: one for the rod and another for the piston, as it can be seen in 2.12.

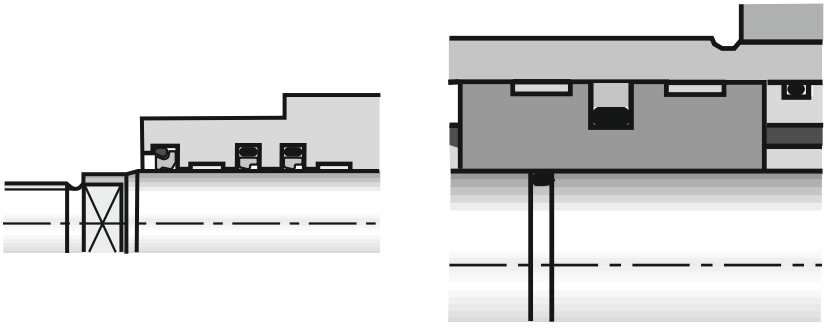

Figure 2.12: Rod and piston seal T-type by Bosch Rexroth

Here, the different materials behave in a different way and so is expected from their effect on the friction.

There are three main types of components:

- O-ring: It is made of elastomer and has a elastic behaviour.
- PTFE components: It is a rigid polimer with much less elastic behaviour.
- Fabric composite: It is rigid and made out of a polymer fabric reinforced with a thermoset matrix.

The figure 2.13 shows a simplified model of how an O-Ring seal responses to the increase of pressure.

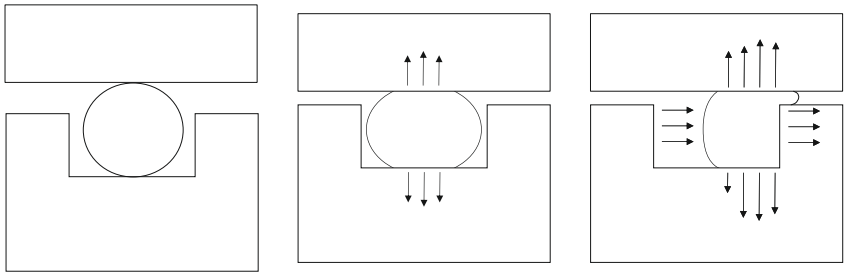

Figure 2.13: O-Ring behaviour when applying pressure

Bosch Rexroth experiment

A experiment carried out by Bosch Rexroth brings an insight into the behaviour of the *fabric composite seals*. The results may be helpful to improve the current model used in this project.

The experiment consisted in a rod driven by an electrical screw spindle through a bearing housing where the bearing strip was placed. The different load over the strip was set by a hydraulic cylinder perpendicular to the rod.

Although the way the pressure over the seal is set is different to the way it would be reached under normal working conditions, it can bring information about the performance of this kind of seals.

The results of the experiment are shown below and can also be found at the report "Performance testing of composite bearing materials for large hydraulic cylinders" [10].

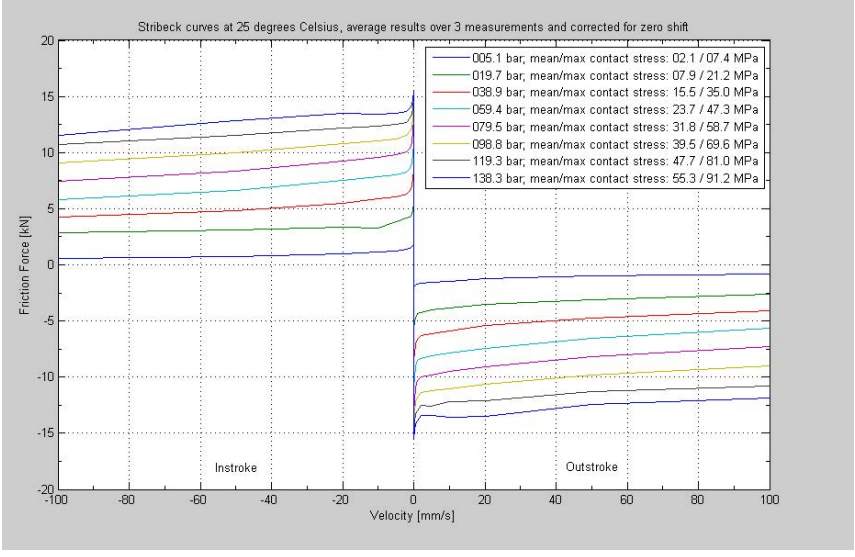

Figure 2.14: Results of the Bosch experiment for fabric composite seals

It can be observed a nearly exponential relation between the load applied to the sealing and the friction force. As well, the increase of the static friction is really significant.

Introducing the values into Matlab, a exponential curve can be obtained to fit the static friction values as it is shown in the figure 2.15

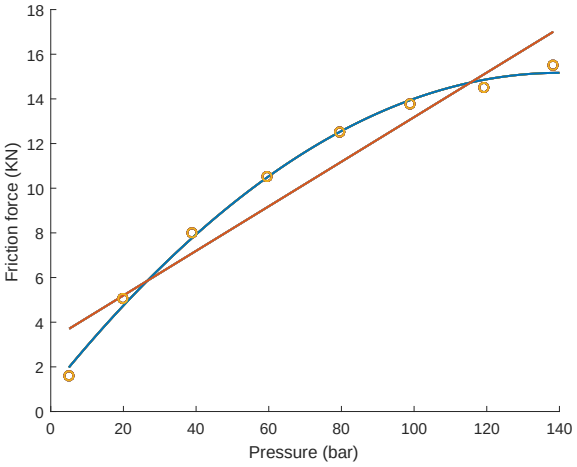

Figure 2.15: Curve fitting for the results of the Bosch experiment

In the figure 2.15, the red and blue lines represent the 1st and 2nd order polynoms that best fit the data from the experiment.

This information must be considered carefully as the conditions and geometry under which the experiment was taken do not match with those which a cylinder will find during its work.

Other experiments

Alternative experiments, however, show different results that may set a difference.

The experiment carried out at the master thesis "Friction Modelling and Parameter Estimation for Hydraulic Asymmetrical Cylinders" [4] performed at Aalborg University, has different results from those obtained in the *Rexroth Bosch* experiment. It is interesting to consider this experiment as it has been developed recreating the normal working conditions, so the data obtained should be directly what this project is looking for.

The experimental analysis was done placing the test cylinder in a bench with a load cylinder which created the different load conditions. Both constant and ramping velocity test were carried out. However, this project will focus on the steady state results (without misleading the ramping data, which may be useful). From the test at different loads, 500 N, 1000 N, 2000 N and 5000 N displayed at 2.16, some values to fill the table 2.1 can be obtained.

These data does not show an obvious evolution of the different parameters as a consequence of the variation of the pressure. However, it can be considered an

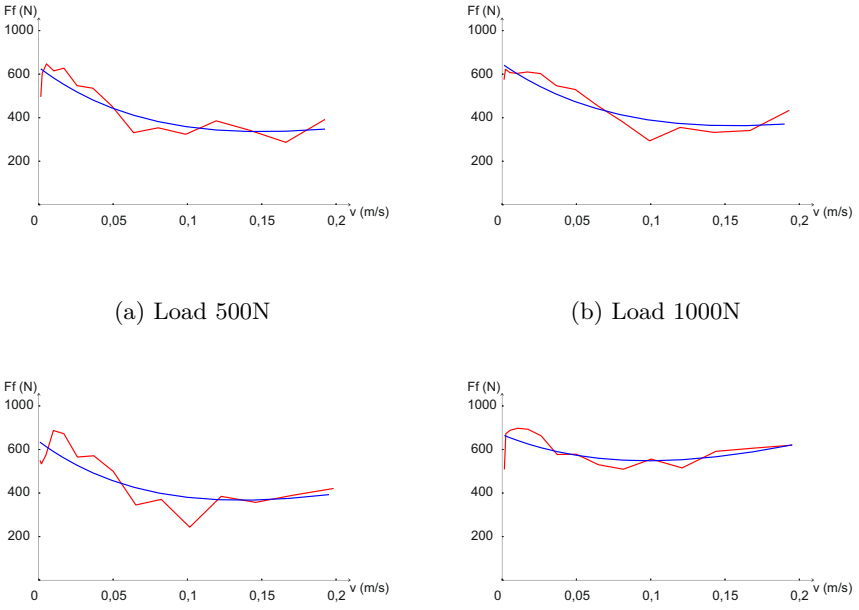

(a) Load 500N

(b) Load 1000N

(c) Load 2000N

(d) Load 5000N

Figure 2.16: Aalborg University's friction experiment for an asymmetric cylinder

Experimental results				
Property	500 N	1000 N	2000 N	5000 N
$F_{stiction}$ (N)	616	647	634	651
$F_{Coulomb}$ (N)	341	379	387	541
$v_{Stribeck}$ ($\mathrm{m\,s^{-1}}$)	0.10	0.11	0.10	0.13

Table 2.1: Aalborg University's friction experiment results

increase of the stiction force as well as the Stribeck velocity (velocity at which the friction force is minimum) for higher loads.

Unfortunately, no quantitative relation between the load and the different parameters can be extracted from the experiment. However, it can be supposed that there is a increase of all the parameters considered: static force, Stribeck velocity and Coulomb friction.

The simplest approach would be to consider a linear relation that, taking into account the few data available, does not have to be worse than a more complex one.

In the figures 2.17a, 2.17b and 2.17c there are shown, again, in red and in blue the 1st and 2nd respectively polynoms that best fit the experimental data.

Outcome

From the experiments mentioned in the previous sections, as well as the theoretical approach, several considerations may be done:

- Both, static friction and Stribeck velocity seem to increase with the load.
- Stribeck curve seems to be much more flat than the theoretical drawings and, consequently, the different regimes more difficult to identify.
- Stribeck velocity can be expected to be reached at aprox. $10\,\mathrm{cm\,s^{-1}}$.
- The region of high friction in the boundary lubrication explained in 2.2.1 does not appear. As it was said, its existence is dependent on the material of the surfaces in contact.
- As both experiments show information from the static regimen till the partial fluid lubrication, the viscous friction cannot be extracted from them.
- The test cylinder employed for previous thesis is asymmetric. As well, the experiment was carried out by setting the necessary pressure in one of the chambers unlike in this project, in which both chambers will be settled at the same pressure. This will have consequences in the number of seals involved in the "load dependent friction proccess". However, this can be adjusted by simply changing the value of the parameters of the possible relation that exists.

Taking this considerations and the equation provided by the LuGre model (2.7), the possible effects of load on the friction can be introduced. This effects are translated in the following relations:

$$\begin{aligned} F_c &= F_c(w) = a_{Fc} + b_{Fc}\, w \\ F_s &= F_s(w) = a_{Fs} + b_{Fs}\, w \\ v_s &= v_s(w) = a_{vs} + b_{vs}\, w \\ \sigma_2 &= \text{cte} \end{aligned} \tag{2.10}$$

Where w represents the load and σ_2 the slope of the viscous friction.

The figure 2.18 shows a simulation of the friction force for equidistant pressures, based on the equations obtained before.

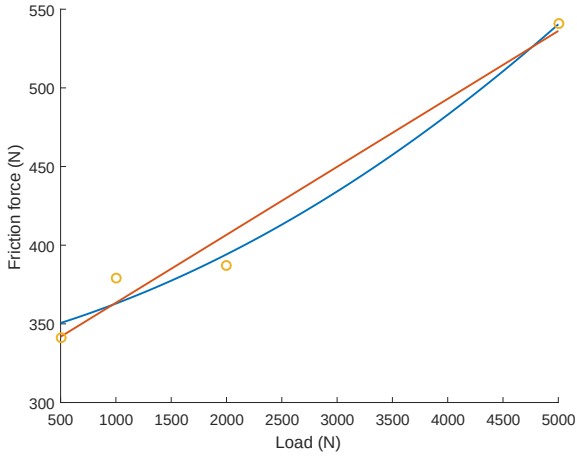

(a) Coulomb friction

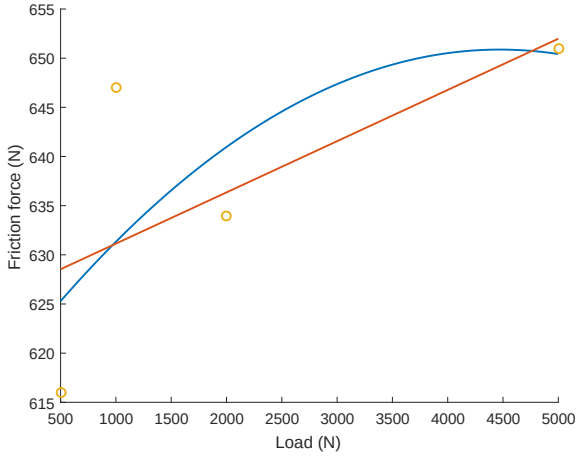

(b) Stiction

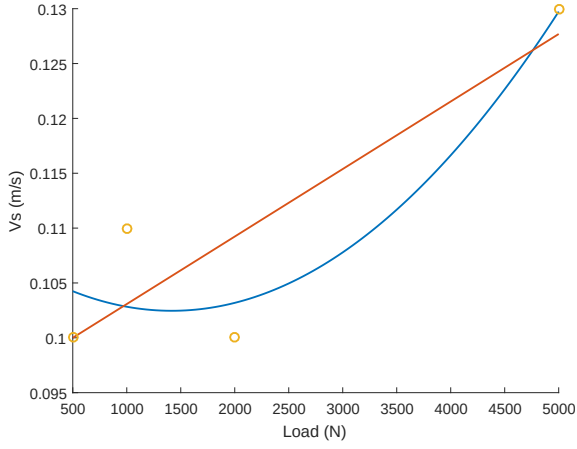

(c) Stribeck velocity

Figure 2.17: Aalborg University's data fitting

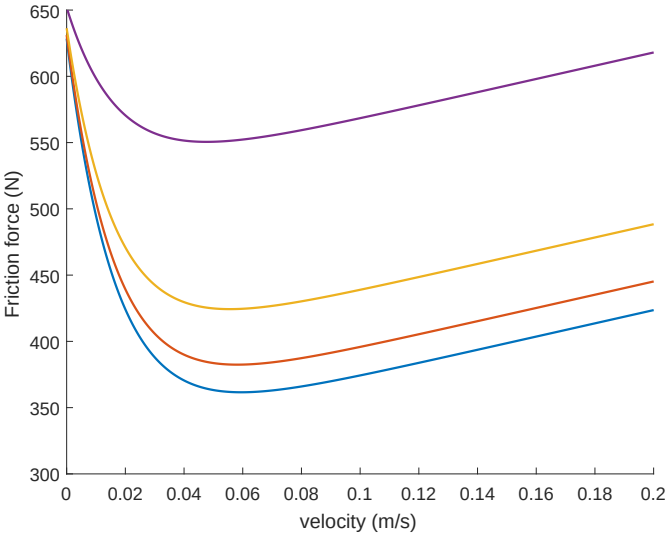

Figure 2.18: Friction simulation for the Aalborg's experiment

Chapter 3

Experimental approach

In the previous chapter it was studied the nature of friction and several theories were introduced. The next step is to perform the necessary experiments in order to analyse, and prove their validity.

For the experiment, a symmetric cylinder provided by *Bosch Rexroth* was tested in a hydraulic bench. To fit it, a platform was specially designed and built using *CAD* software and with the help of the people from the workshop.

3.0.1 Experiment

The experiment tries to determine the friction forces that occur when the test cylinder works at different pressures as well as at different velocities.

The equipment employed to this purpose is an universal testing machine from MTS model: *858 Mini Bionix*, mainly used to carry out tensile testing. This machine allows to set the wanted working conditions for the cylinder.

The experimental assembly consists on the cylinder (1), the universal testing machine (2), the support structure (3), a load cell (4) and a manual hydraulic pump (5).

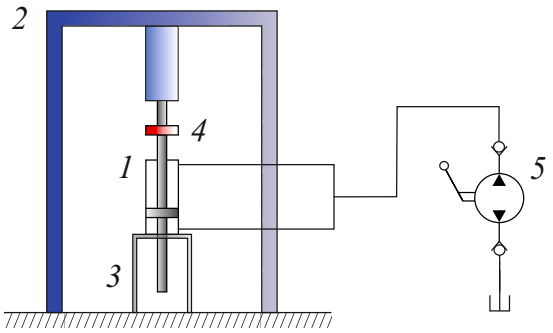

Figure 3.1: Experiment assembly

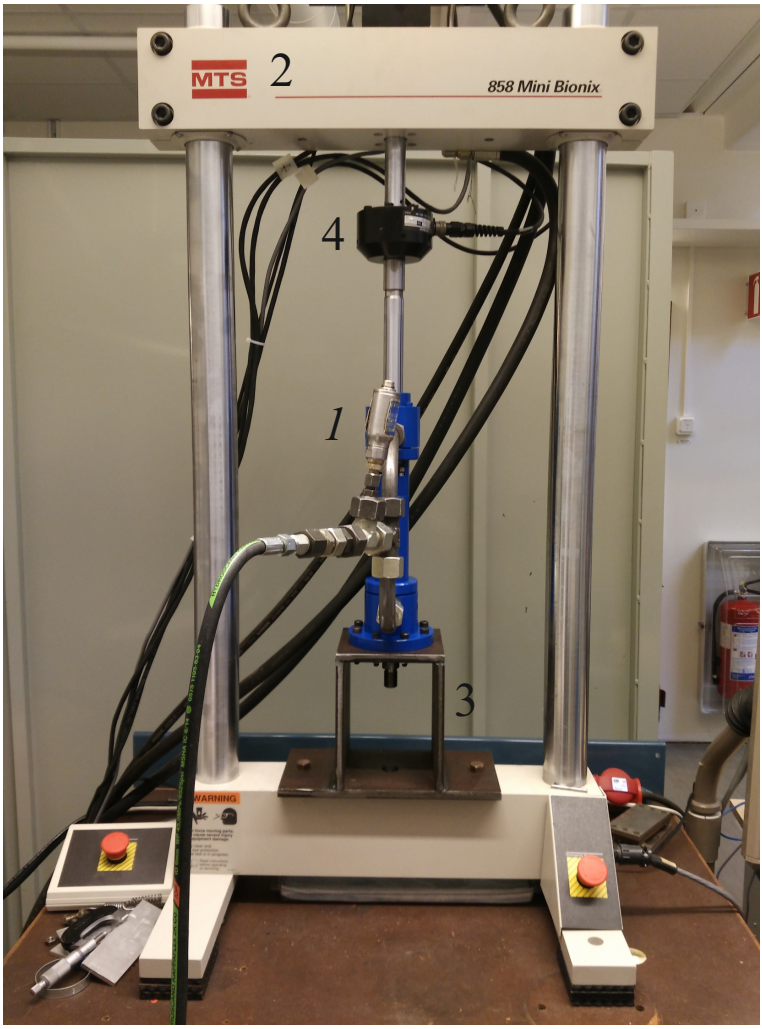

Figure 3.2: Laboratory experimental assembly

Figure 3.3: Laboratory experimental assembly with manual pump

Once these elements are properly assembled, the experiment can be carried out and the focus may be placed in the force equations:

$$\begin{aligned} \ddot{x}\,(m_p + m_{lc}) &= A_1 p_1 - A_2 p_2 + F_l - F_f \quad \text{if } v > 0 \\ \ddot{x}\,(m_p + m_{lc}) &= A_1 p_1 - A_2 p_2 + F_l + F_f \quad \text{if } v < 0 \end{aligned} \tag{3.1}$$

The sgn function can be introduced here in order to avoid sign changes:

$$\ddot{x}\,(m_p + m_l c) = A_1\, p_1 - A_2\, p_2 + F_l - F_f\, \mathrm{sgn}(v) \tag{3.2}$$

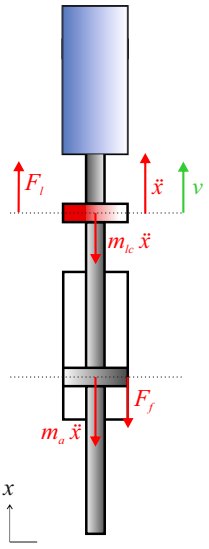

Figure 3.4: Free body diagram

Where:

F_f	friction force
m_p	mass of the cylinder rod
m_{lc}	mass of the load cell
$\ddot{x}$	acceleration of the system
A_1	area of the piston in the chamber 1
A_2	area of the piston in the chamber 2
p_1	pressure in the chamber 1
p_2	pressure in the chamber 2
F_l	force applied by the machine

If the experiment is carried out in steady state ($\ddot{x} = 0$), taking into account that the cylinder is symmetric ($A_1 = A_2$) and considering the possibility that the pressure in both chambers can be setted the same ($p_1 = p_2$), most of the terms of the equation disappear, showing the friction force as equal to the load applied by the machine. Consequently, the data provided by the load cell shows directly the friction force itself.

3.0.2 Experiment design

As it was seen before, in order to determine the friction so that the data can be analysed, the experiment must be done under steady state conditions (constant velocity). This implies setting an acceleration period in which the machine will reach the desired velocity and during which the data will not be considered. In addition, the construction of the cylinder makes it necessary to also notice the *cushioning* that affects at the end of the stroke.

In order to simplify the data analysis, this period is set as the longer time that the machine requires to reach the constant velocity of all the working conditions. Considering the formulas provided in the previous sections, this time is expected to be higher with higher pressure and also at higher velocities due to the time that it takes to reach them, this is shown at the figure 3.5.

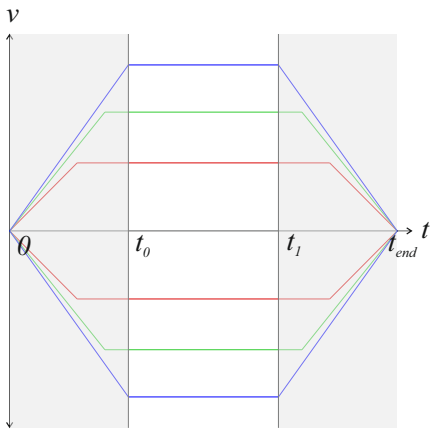

Figure 3.5: Shape of the data expected to consider

The desired data is located between t_0 and t_1. As a consequence of the discrete nature of these data, the procedure has to consider the position of the element in the vector instead of the time (see figure 3.6).

Due to the limit in the size of the data that can be gathered in each file, the time interval between measurements has to be modified depending on the total time each experience lasts. For the 2 slower velocities, this time is set to 20 ms, bringing about an amount of 10,001 discrete values for the $1\,\mathrm{mm\,s^{-1}}$ speed. For the remaining ones, the time interval is set to 10 ms in order to achieve the highest accuracy possible.

As a consequence of the old software employed to control the machine and gather the data: *Windows NT*, its acquisition and managing process presented several difficulties. For each velocity, the program had to be introduced again, bringing about a new .txt file with the corresponding data mixed with string characters. Considering the average of 27 different speeds at which the experience has been

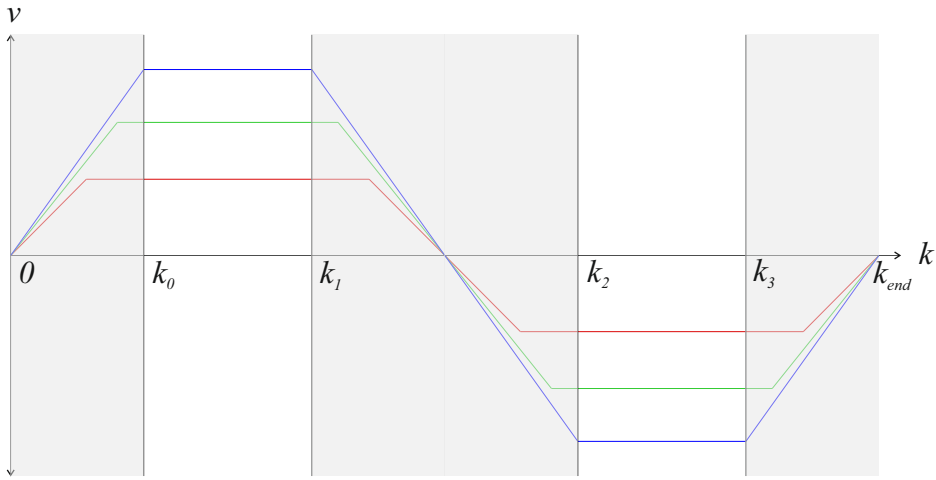

Figure 3.6: Discretization of the data and analysis

carried out and the 10 different pressures, this brings about 270 .txt files to analyse and manage.

A *Matlab* script was created in order to deal with the amount of files and the difficulties to read through them.

After analysing the data and the evolution of the curves through the time, the decision is to omit the 10 first elements on each movement (descending/ascending), this leads to set $k_0 = 10$, $k_1 - k_2 = 20$ and $k_{end} - k_3 = 10$ (see figure 3.6).

The real shape of the data is sown at figure 3.7, where it can be observed the variation of the friction force at the beginning and end of the stroke. For the first figure, the interval between measurements is 20 ms, showing a total duration of the experience of 200 s. In the second one, the interval is set to 10 ms, this means a total duration of 34 s.

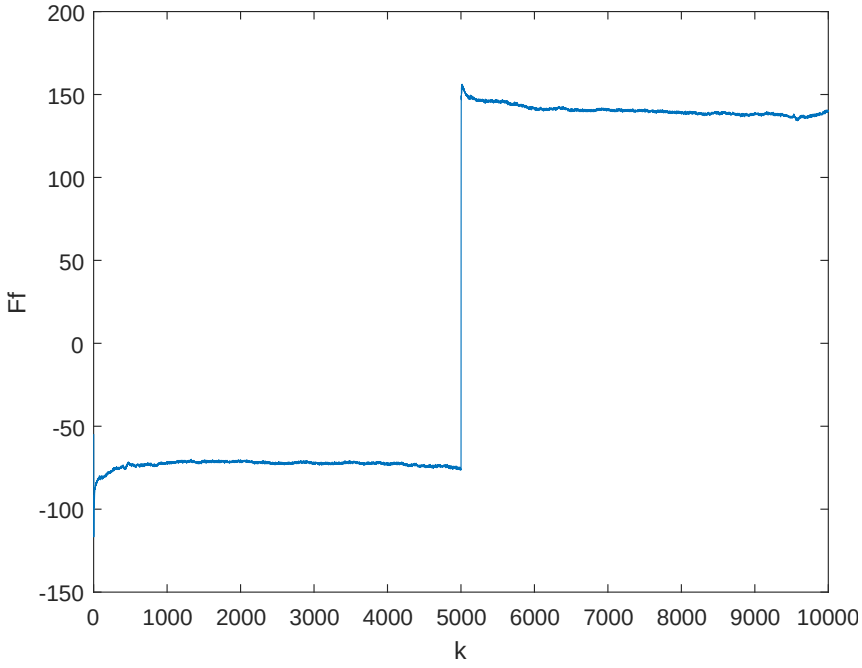

(a) $1\,\mathrm{mm\,s^{-1}}$

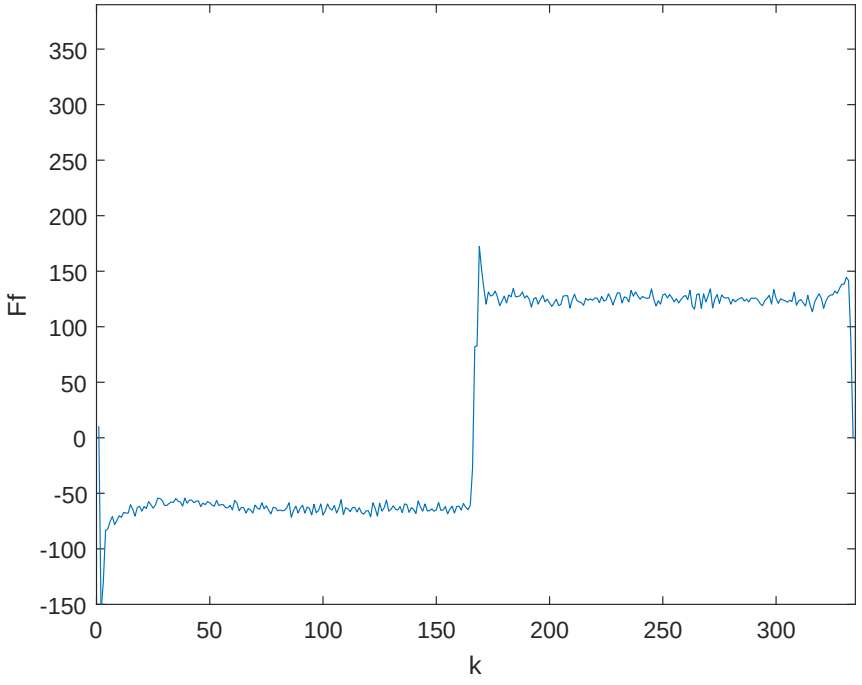

(b) $135\,\mathrm{mm\,s^{-1}}$

Figure 3.7: Real data shape for different velocities. Discrete values

Chapter 4

Results

With reference to the LuGre model at steady state, described in the equation 2.7, which is used as the reference point for this project.

$$F_f = F_c + (F_s - F_c)e^{-\left(\frac{v}{v_r}\right)^{\alpha}} + \sigma_2\, v \qquad \text{(2.7 rev)}$$

The pressure dependence of the parameters Fs, Fc, and σ_2 can be accurately stated after analysing the data obtained, as it is shown in the next pages.

$$F_c = F_c(p) = 70,2 + 0,5\, p \tag{4.1}$$

$$F_s = F_s(p) = 112.9 + 0,6\, p \tag{4.2}$$

$$\sigma_2 = \sigma_2(p) = 0.34 + 8 \cdot 10^{-4}\, p \tag{4.3}$$

Where F_c and F_s are given in N, σ_2 is given in $\mathrm{N\,s\,mm^{-1}}$ and p is given in bar.

On the other hand, α, v_r, and the Stribeck velocity (v_s) do not appear to have any relation with the pressure. In addition, the high variance of these parameters makes it difficult to choose an appropriate value, leading to an estimated range of them.

In the sections 4.1.1 and 4.1.2 it is showed how by fixing the values of $\alpha = 1$ and $v_r = 10\,\mathrm{mm\,s^{-1}}$ an accurate and simple model can be obtained.

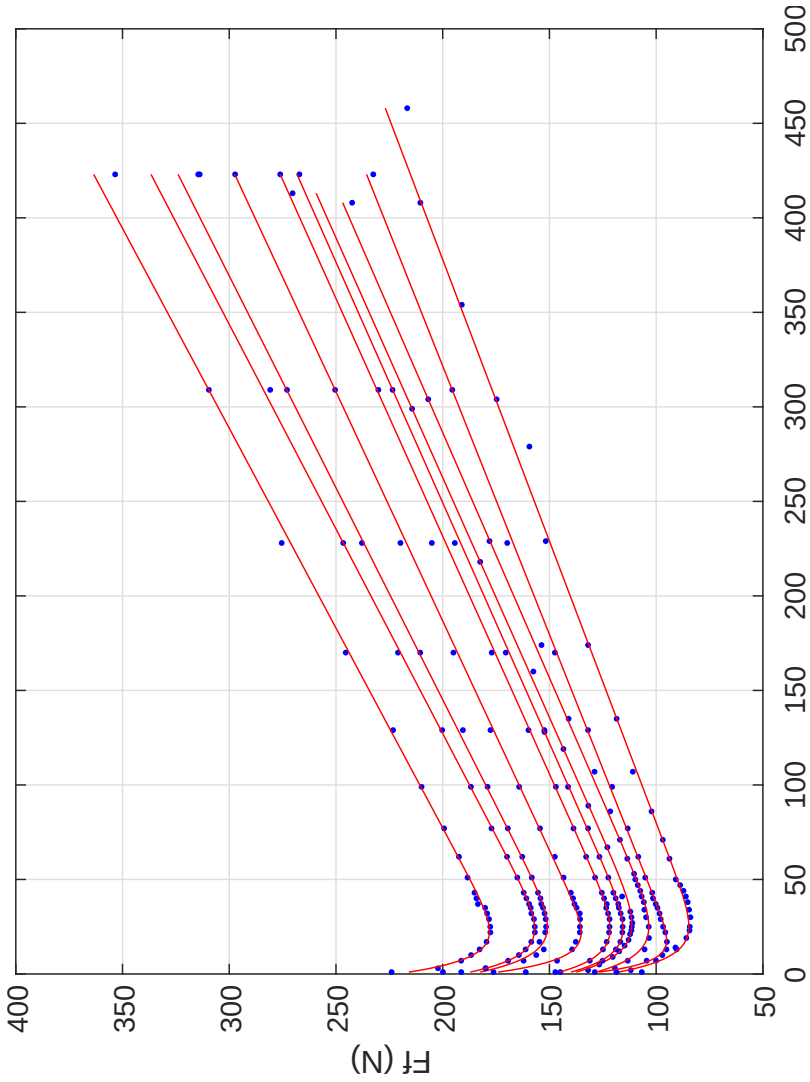

Figure 4.1: Experimental data fitting. Equispaced pressures from 0.1 to 159 bar

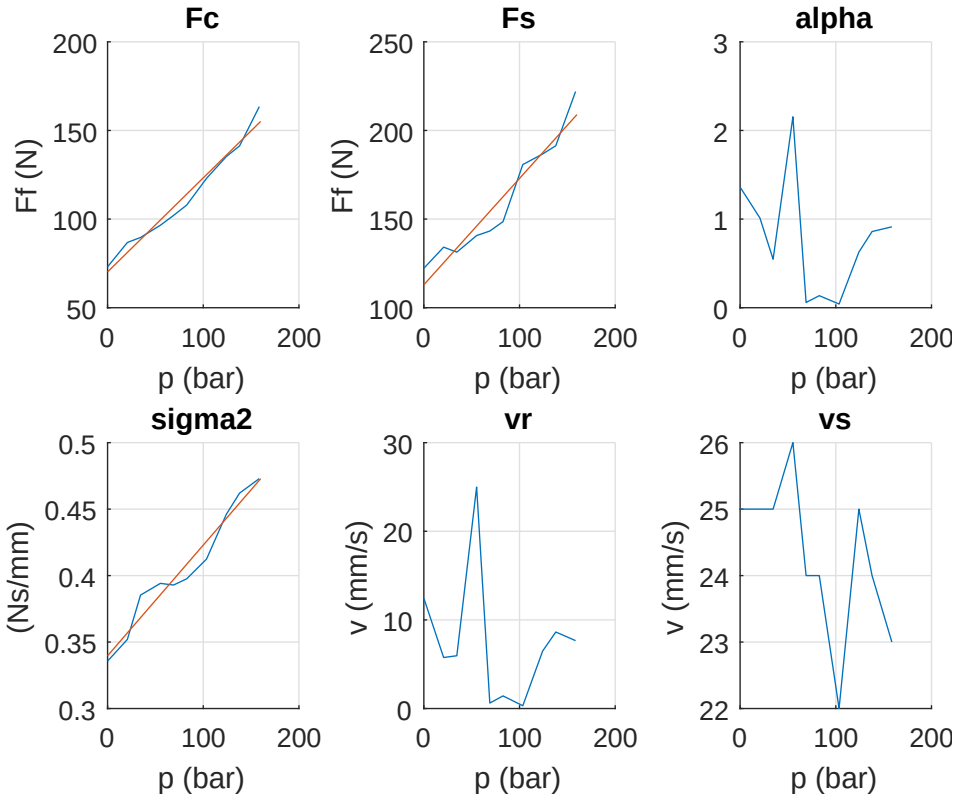

Figure 4.2: Parameter variation with the pressure

This pressure dependence can be observed in the figure 4.2. As well, some numeric values are given in the table 4.1.

Experimental results					
Property	0 bar	55 bar	83 bar	124 bar	159 bar
$F_{stiction}$ (N)	113.0	146.0	162.6	187.4	208.1
$F_{Coulomb}$ (N)	70.2	99.5	114.1	136.0	158.6
σ_2 ($\mathrm{N\,s\,mm^{-1}}$)	0.340	0.386	0.398	0.409	0.472
$v_{Stribeck}$ ($\mathrm{mm\,s^{-1}}$)	25	26	24	25	23

Table 4.1: Results of the experiment

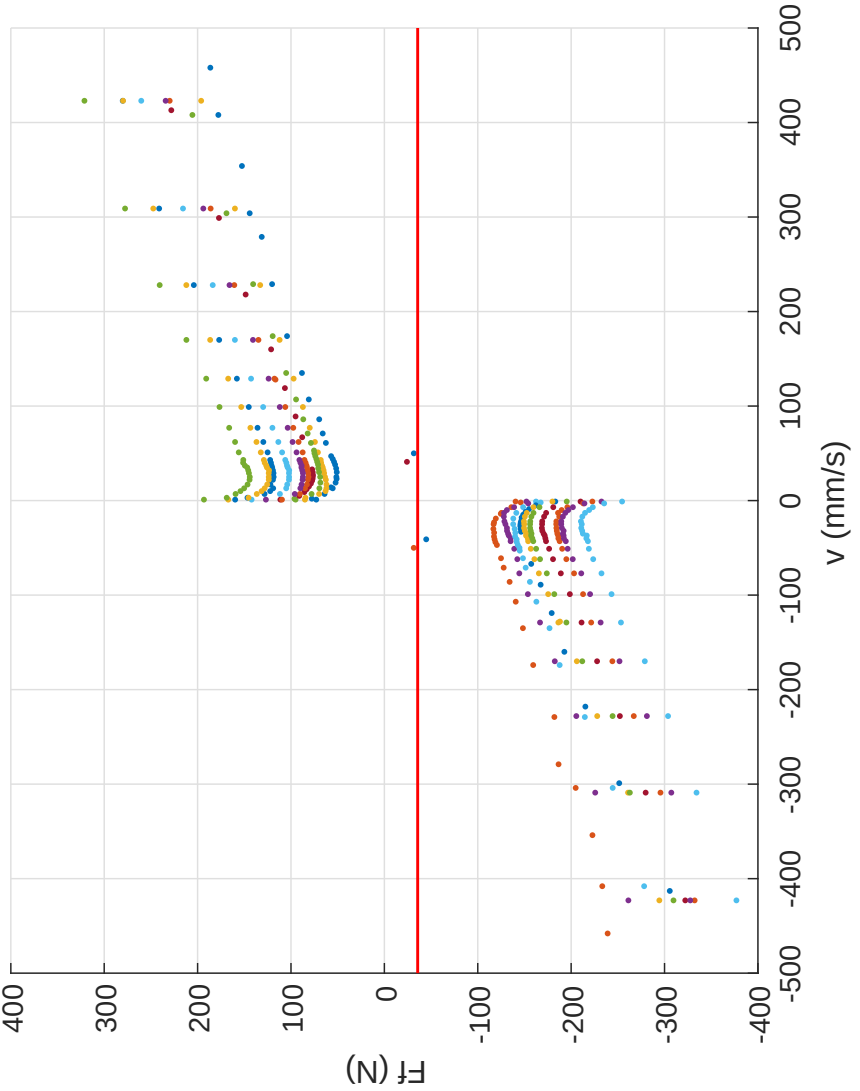

Figure 4.3: Results of the experiment and constant data displacement. Equispaced pressures from 0.1 to 159 bar

From the figure 4.3, it can be seen the influence of the weight of the load cell. The displacement of the data in the descending movement compared with the ascending one can be measured as a constant value of $-35.67\,\mathrm{N}$, represented by a red line.

4.1 Influence of other parameters

As it was seen in the figure 4.2, the parameters α and v_r show no obvious dependence on the pressure. For α, different values are suggested according to different bibliography. While [12] indicates a value of 1, [13] introduces a range between 0.5 and 1, and [14] considers a value of 2.

Due to the variance obtained through the experiment and the disagreement when consulting different authors, it may be interesting to analyse the influence of this parameter in the overall friction.

As well, v_r shows also a high variance. By analysing its dimensions $[\mathrm{L}][\mathrm{T}]^{-1}$ and the effect on the shape of the curves, it can be deduced its relation with the *Stribeck velocity* as some authors suggest. However, although some literature introduces directly v_r with the name of v_s, from the experiment performed for this thesis it can be observed that they do not exactly correspond (see figure 4.2). For this parameter, a value of $10\,\mathrm{mm\,s^{-1}}$ could be reasonable considering the results obtained and the statements of other authors [4].

However, before any further simulation, based on the mean of the experimental data, there can be suggested the values of $\alpha = 0.77$ and $v_r = 7.43\,\mathrm{mm\,s^{-1}}$.

4.1.1 Influence of α

The first parameter to analyse is α. Its influence on the friction can be observed by simulating with different values.

The first values considered are those suggested from the literature: 0.5, 1, 1.5 and 2.

In order to determine whether fixing a value is reasonable although the high variance shown when fitting the curves, the Squared Mean Error (SME) is used.

This is introduced by the following formula:

$$\mathrm{SME} = \sqrt{\mathrm{mean}\left(F_f - F_f'\right)^2} \tag{4.4}$$

The different α values bring about curves that are shown at the end of this chapter.

These simulations show how α strongly influences the shape of the curves. It can be seen how, for higher α values, the Stribeck effect is more sharp. As well, although it cannot be clearly seen, the constant friction force period just before the static friction that was mentioned in 2.3 appears with bigger α values.

A SME analysis will show the goodness of the simulation compared with the experimental results. The table 4.2 shows the value of this errors for $v_r = 7.43\,\mathrm{mm\,s^{-1}}$.

Errors	
α	SME
0.5	6.544
0.77	5.064
0.8	4.986
1	4.722
1.5	4.864
2	5.1465

Table 4.2: Evaluation of the errors. α variable, $v_r = 7.43\,\mathrm{mm\,s^{-1}}$

From here, it can be seen that the lower error comes with an $\alpha = 1$ although the mean of the experimental data is 0.77. As well, by analysing the results for v_r =10 $\mathrm{mm\,s^{-1}}$ it can be seen that, although the average error is bigger, the minimum, which is the interesting one in order to chose a right value is smaller.

Errors	
α	SME
0.5	7.026
0.77	5.2340
0.8	5.1165
1	4.639
1.5	4.8643
2	4.9821

Table 4.3: Evaluation of the errors. α variable, $v_r = 10\,\mathrm{mm\,s^{-1}}$

4.1.2 Influence of v_r

The other parameter with influence on the friction is v_r. By setting an alpha value of 1 (which was seen to generate the lower error) and varying v_r around the previously stated value of $10\,\mathrm{mm\,s^{-1}}$, some plots can be generated (see figures at the end of the chapter).

From these figures it can be seen how v_r directly affects the *Stribeck velocity* although not corresponding with the same value.

By analysing the error values, the table 4.4 can be constructed.

Errors	
v_r	SME
5	11.878
7.43	4.722
10	4.639
15	6.2135

Table 4.4: Evaluation of the errors. v_r variable, $\alpha = 1$

An interesting result is shown: considering the experimental mean value for α and v_s does not generate the minimum error, but another value does.

From the previous lines, it can be stated that the use of fixed parameters for α and v_r provides a reasonable and accurate result. The suggested values for these are $\alpha = 1$ and v_r $10\,\mathrm{mm\,s^{-1}}$.

Considering the following figures, the ones with variable α are simulated for a constant v_r of $10\,\mathrm{mm\,s^{-1}}$. Consequently, when varying v_r, the corresponding plot for $\alpha = 1$ and $v_r = 10\,\mathrm{mm\,s^{-1}}$ can be omitted because of being redundant.

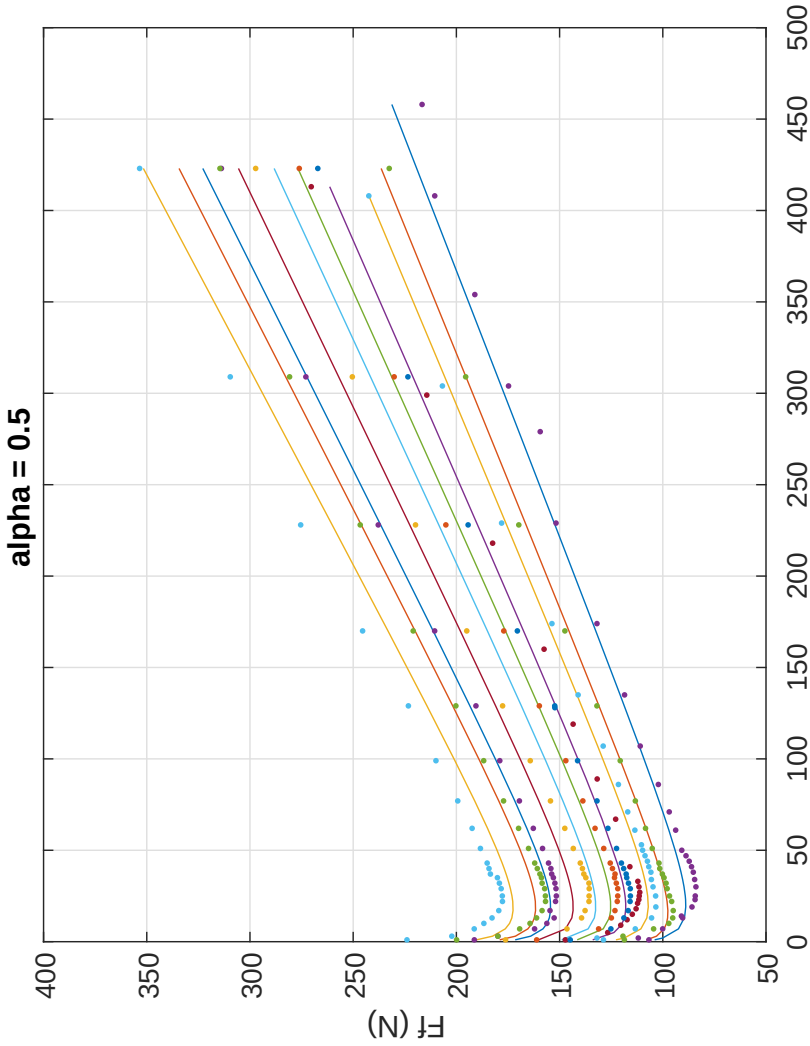

Figure 4.4: Simulation for $\alpha = 0.5$ compared with experimental results

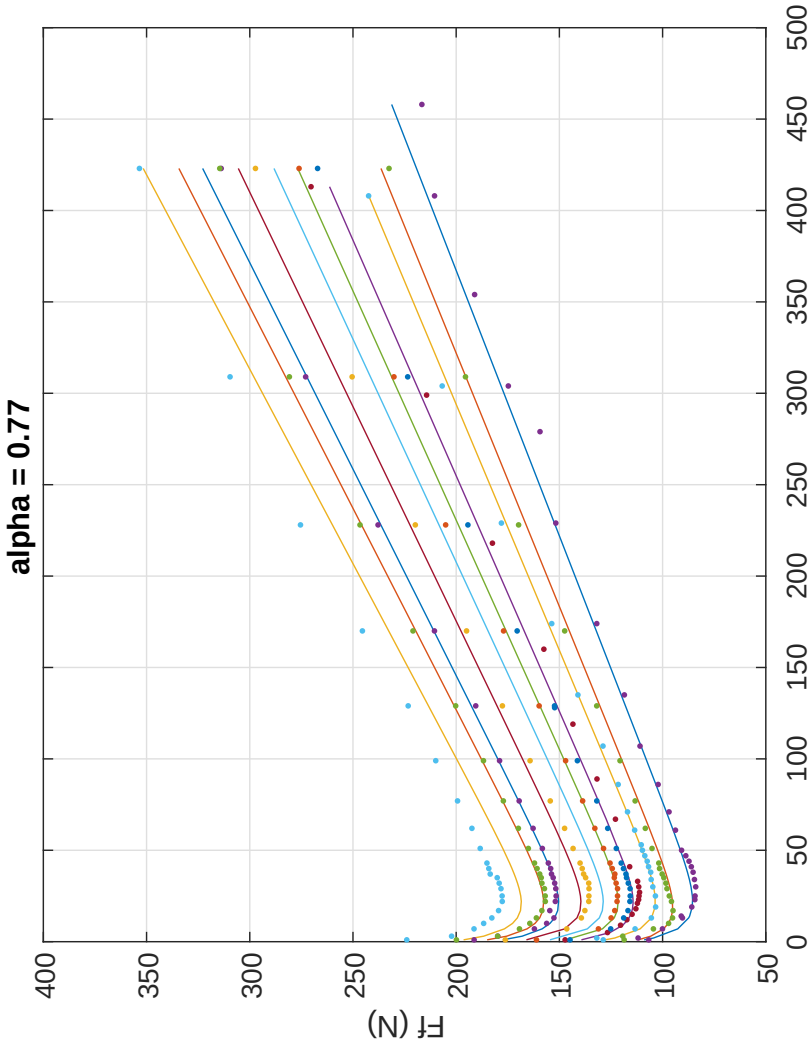

Figure 4.5: Simulation for $\alpha = 0.77$ compared with experimental results

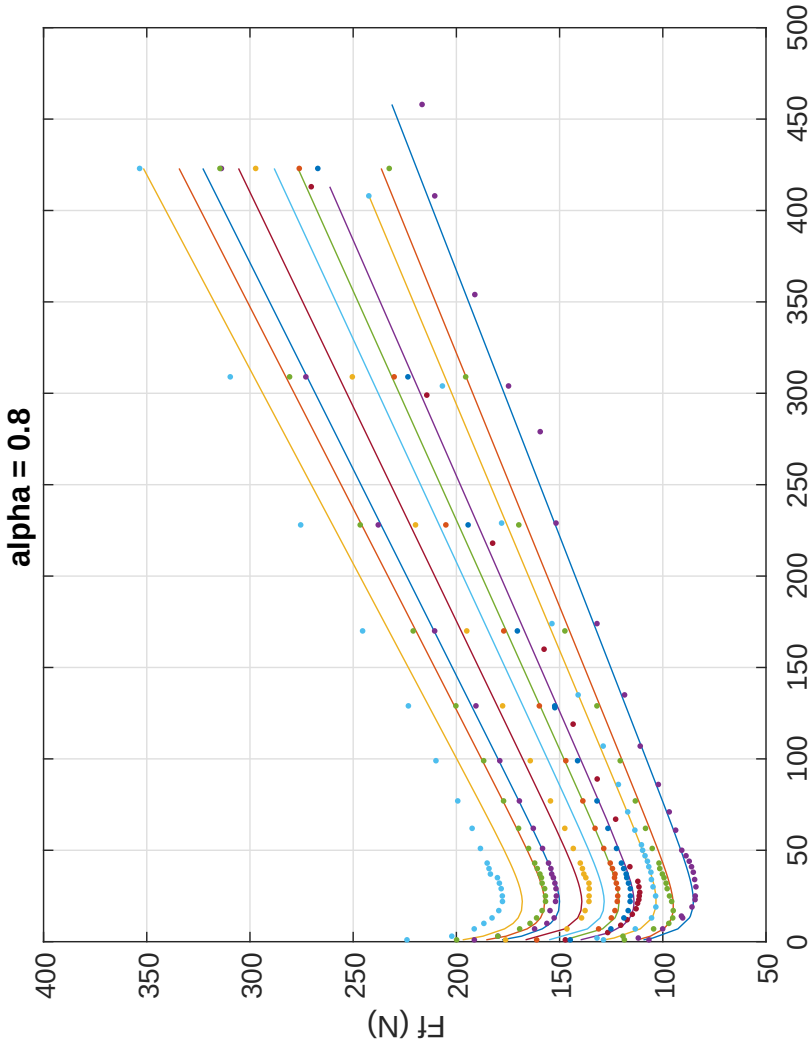

Figure 4.6: Simulation for $\alpha = 0.8$ compared with experimental results

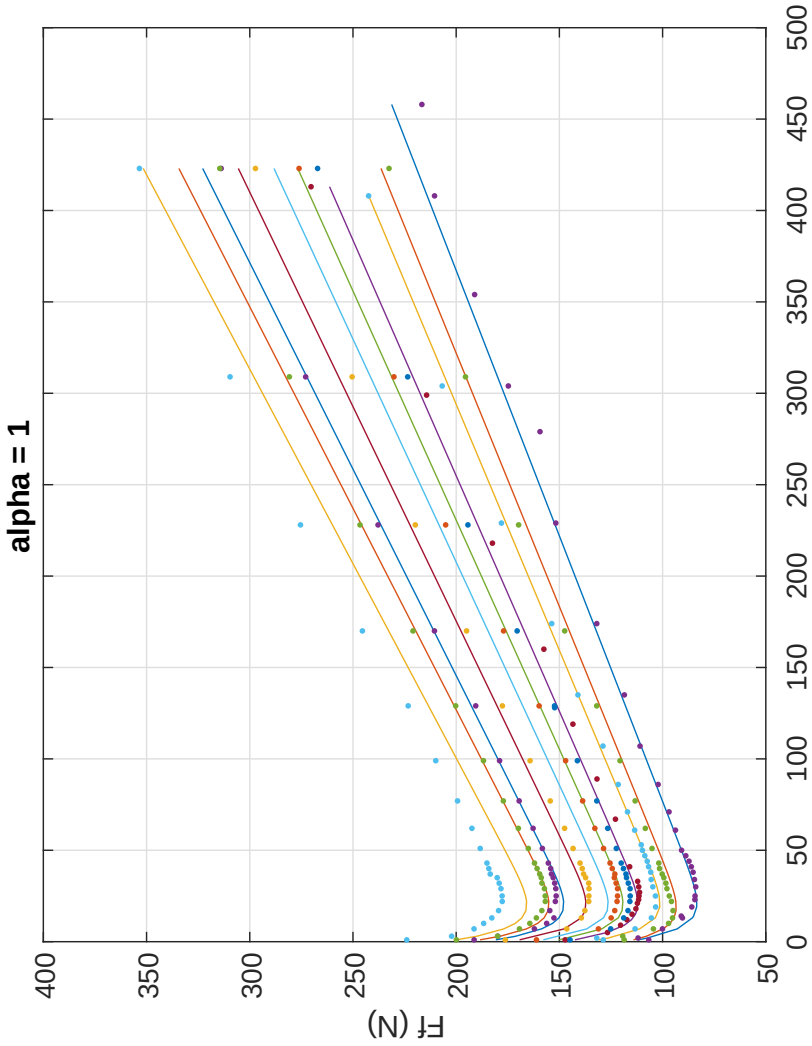

Figure 4.7: Simulation for $\alpha = 1$ compared with experimental results

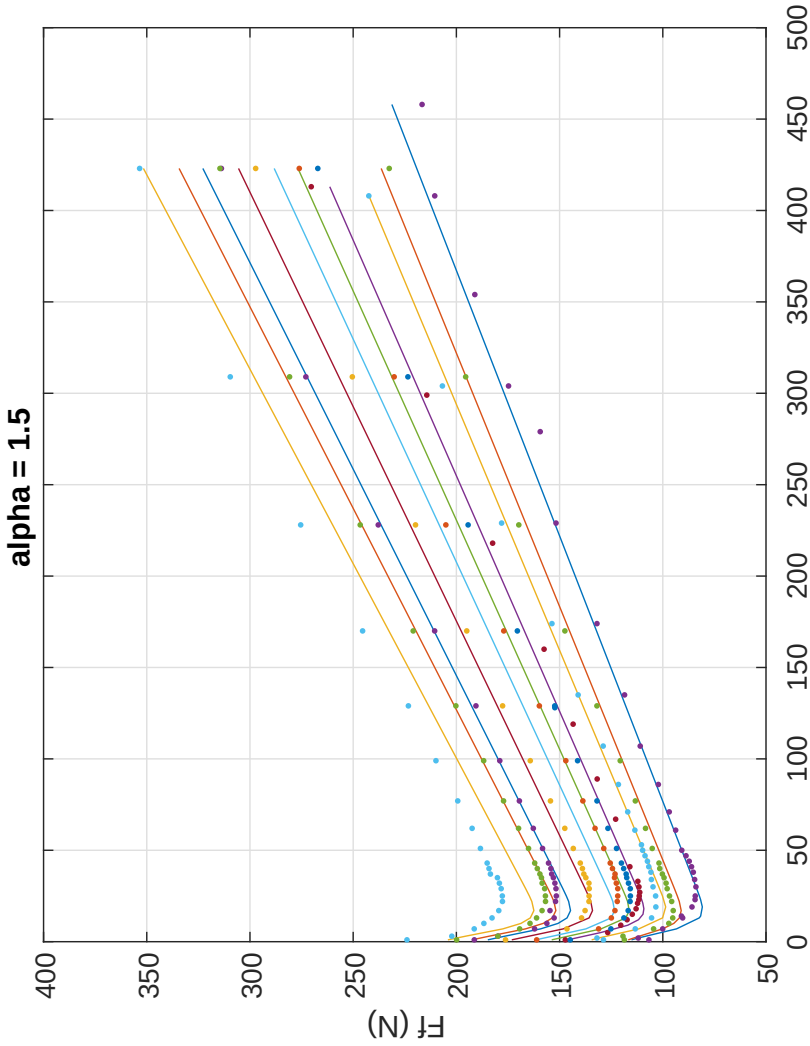

Figure 4.8: Simulation for $\alpha = 1.5$ compared with experimental results

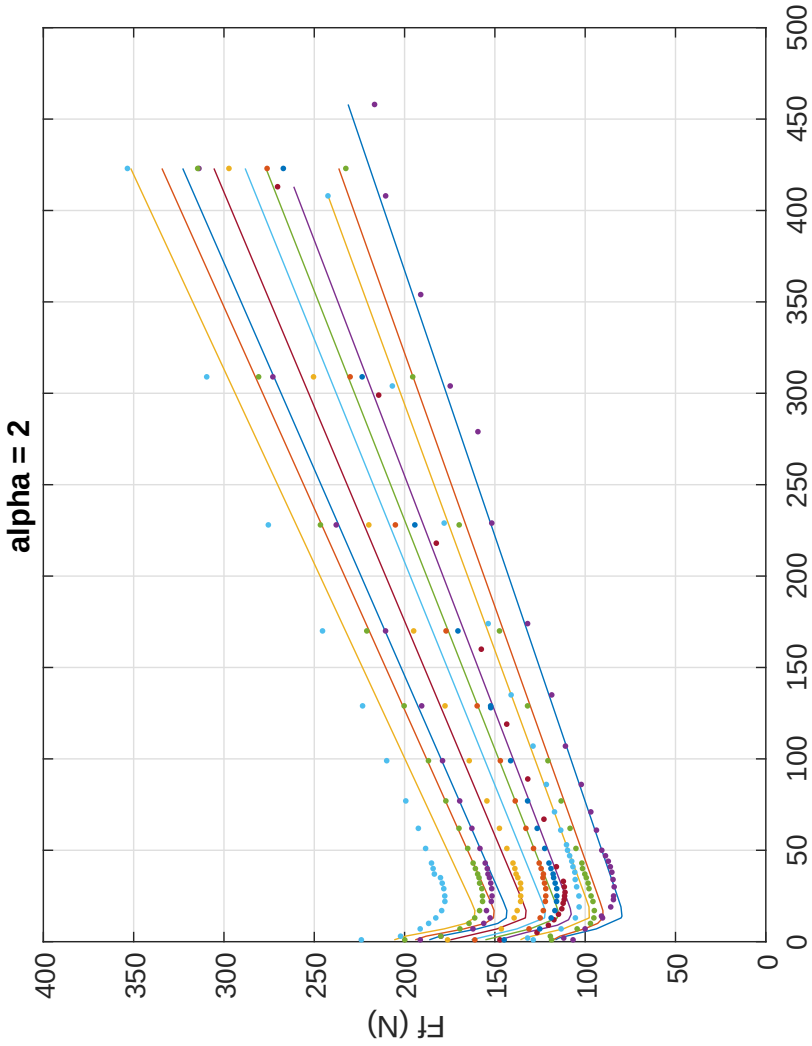

Figure 4.9: Simulation for $\alpha = 2$ compared with experimental results

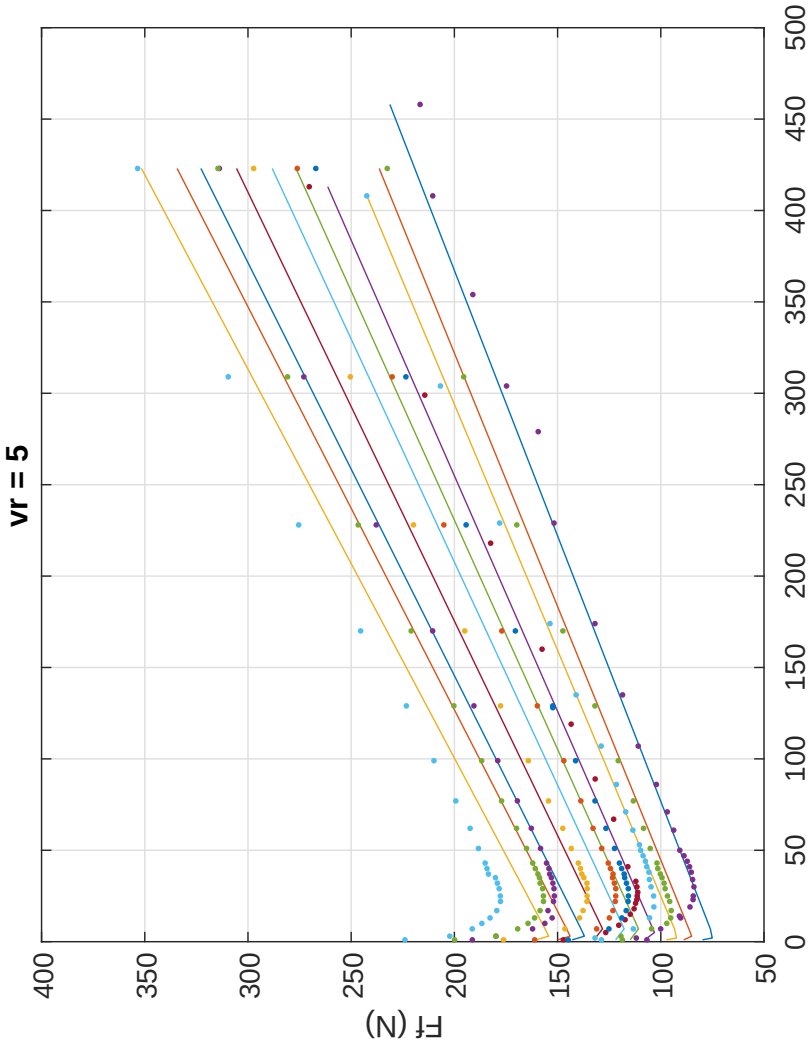

Figure 4.10: Simulation for $v_r = 5\,\mathrm{mm\,s^{-1}}$ compared with experimental results

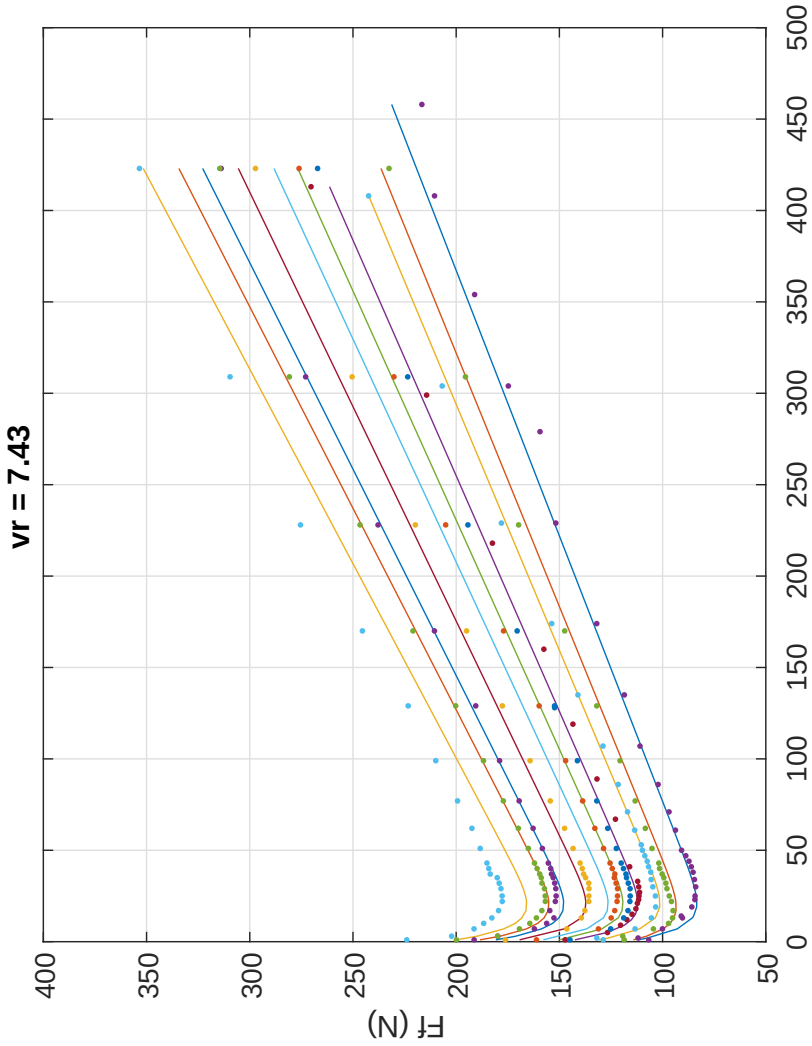

Figure 4.11: Simulation for $v_r = 7.43\,\mathrm{mm\,s^{-1}}$ compared with experimental results

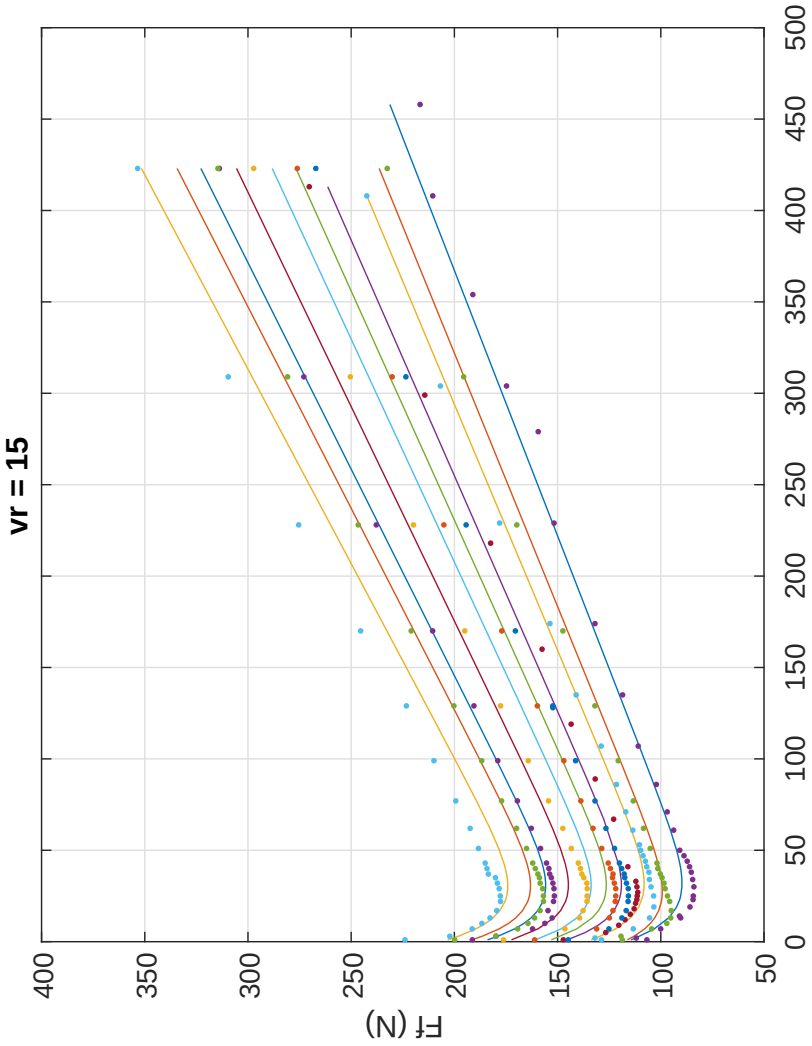

Figure 4.12: Simulation for $v_r = 15\,\mathrm{mm\,s^{-1}}$ compared with experimental results

Chapter 5

Conclusion

According to the first aim of this thesis: determine the factors that affect friction, a strong correlation between the friction force, velocity and pressure can be stated. Whereas the velocity was already known to affect the friction and several models do consider it, pressure is a frequently forgotten factor which has been proved to strongly affect the friction phenomena.

As it is introduced in the chapter 4, the following model considering both: velocity and pressure, can be stated.

$$F_f = F_c + (F_s - F_c)\, e^{-\left(\frac{v}{v_r}\right)^{\alpha}} + \sigma_2\, v \qquad \text{(2.7 rev)}$$

With the parameters Fs, Fc, and σ_2 as:

$$F_c = F_c(p) = 73,5 + 0,5\, p \qquad \text{(4.1 rev)}$$

$$F_s = F_s(p) = 117 + 0,6\, p \qquad \text{(4.2 rev)}$$

$$\sigma_2 = \sigma_2(p) = 0.34 + 8 \cdot 10^{-4}\, p \qquad \text{(4.3 rev)}$$

As well, the fixed values for the parameters $\alpha = 1$ and $v_r = 10\,\mathrm{mm\,s^{-1}}$ have proved to provide an accurate and simple model.

The second research question can not been answered without analysing a big amount of cylinders. Further experiments would be required in order to generate valid conclusions that enable predicting the behaviour of a variety of cylinders. However, a suggestion can be made to the cylinder providers:

As the pressure has its effect on the seals and the number of models is limited within the same company, a standardised procedure to test them could be implemented in order to provide the customers with valuable information. By just indicating the parameters stated before: $F_c(p)$, $F_s(p)$, $\sigma_2(p)$, α and v_s, a deep knowledge about the performance of the cylinder can be acquired and, consequently, the selection of the cylinder facilitated. Apart from the characteristics of the seals, the size and other features of the cylinder may be easily considered by introducing scale factors in order to compensate the increase of sliding surface.

Chapter 6

Discussion

The experiment has provided really valuable information to understand the behaviour of the friction phenomena at different velocities and its dependence on the pressure.

The quality of the data and its similarity to the model stated by the LuGre equations support also the reliability of this model.

With reference to the summary model suggested in 2.3, some modifications can be done. However, there are shown the reasonable similarities and quality of this assumption taking into account the lack of initial data.

The increase of friction force with pressure was an initial assumption and has been clearly displayed as well as the increase of the stiction force. Other considerations previously mentioned as the initial decreasing of friction force from the beginning of the movement, without displaying the stabilized transition during the boundary lubrication regimen, is also noticeable from the results.

Although the parameters analysis explains a homogeneous distribution of the lines as the pressure increases, by observing the real data (see figure 4.1), it can be seen that the curves are not evenly distributed. In addition, the 2nd curve associated with the 20.7 bar shows an strange Stribeck effect. The previously studied influence of pressure and velocity, as well as the LuGre parameteres (chapter 4), cannot explain this behaviour, so other factors must be considered.

The experiment was carried without any **temperature** control. Considering the long working cycles, this is a hypothesis worth considering.

In addition, some measurements taken under the same working conditions showed different results. When performing continue experiments, the later experiences and, hence, those for which the system could be warmer, proved lower friction force. This may be explained considering the decrease of viscosity of the lubricant with temperature. According to the Hersey number (see 2.8) this increase of viscosity would allow the development of the lubricant film at lower velocity, reducing the Stribeck velocity and the friction force in general.

As well, the **wear of the seals**, although could not be studied in for this thesis, is a probable factor that will affect the behaviour of the friction forces.

Due to the lack of time, it has not been possible to perform the experiment with the other cylinder provided by *Bosch Rexroth* that incorporates normal seals, opposing the *low friction* ones from the current object of study. It would have been of special interest in order to observe the behaviour of the parameters depending on the kind of sealing so that a global understanding of different cylinders can be achieved.

For a future project, the study of a different cylinder with different seals, as well as a more strict control on the temperature effects while performing the experiment, could be an interesting topic to bear in mind.

Bibliography

[1] H. Olsson, K. J. Åström, C. :Canudas de Wit, M. Gäfvert, P. Lischinsky, *Friction Models and Friction Compensation*, 1997.

[2] F. Al-Bender, *Fundamentals of friction modeling*, Katholieke Universiteit Leuven, 2005.

[3] B. Armstrong-Hélouvry, P. Dupont, C. Canudas de Wit, *A survey of models, Analysis Tools and Compensation Methods for the Control of Machines with Friction*, Automatica, Vol. 30, No. 7, 1994.

[4] M. Hvoldal, C. Olesen, *Friction Modelling and Parameter Estimation for Hydraulic Asymmetrical Cylinders*, Master Thesis, Aalbort University, 2011.

[5] K. J. Ström, C. Canudas de Wit, *Revisiting the LuGre friction model*, IEEE Control Systems Magazine, Institute of Electrical and Electronics Engineers, 2008.

[6] M. Hakan Turhan, *Systemidentification and Adaptive Compensation of Friction in Manufacturing Automation Systems*, Master Thesis, Master of applied Science in Mechanical Engineering, University of Waterloo, 2013.

[7] T. Mang, K. Bobzin, T. Bartels, *Industrial Tribology: Tribosystems, Friction, Wear and Surface Engineering, Lubrication*, 2011.

[8] S. Shaffer, *Generating a Stribeck Curve in a Reciprocating Test*, Bruker Corporation, Application Note #1004, USA, 2014.

[9] D. Chou, *Dahl Friction Modelling*, Thesis, Department of Mechanical Engineering, Massachusetts Institute of Technology, 2004.

[10] *Performance testing of composite bearing materials for large hydraulic cylinders*, Bosch Rexroth Corporation, USA, 2014.

[11] H. van Leeuven, *Engineering Tribology*, Proc.1 MechE Vol.223 PartJ:J. Hamburg, Germany, 2009.

[12] A. Tustin. *The effects of backlash and of speed-dependent friction on the stability of closed-cycle control systems.* Journal of the Institution of Electrical Engineers Part 1 General, 94:143-151, 1947.

[13] L. C. Bo and D. Pavelescu, *The friction-speed relation and its influence on the critical velocity of the stick-slip motion.* Wear, 82(3):277-89, 1982.

[14] B. Armstrong-Hélouvry, *Control of Machines with Friction.* Kluwer Academic Publishers, Boston, Ma., 1991

Appendix A

Support structure planes

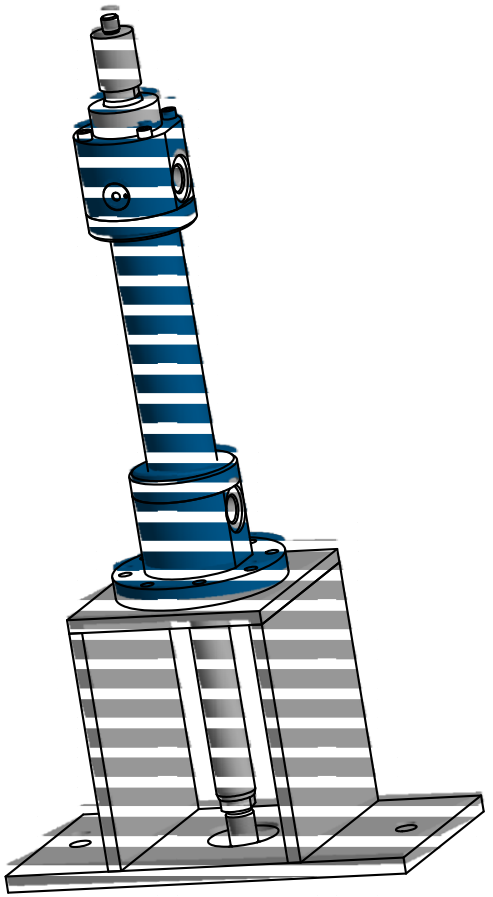

E 1:3

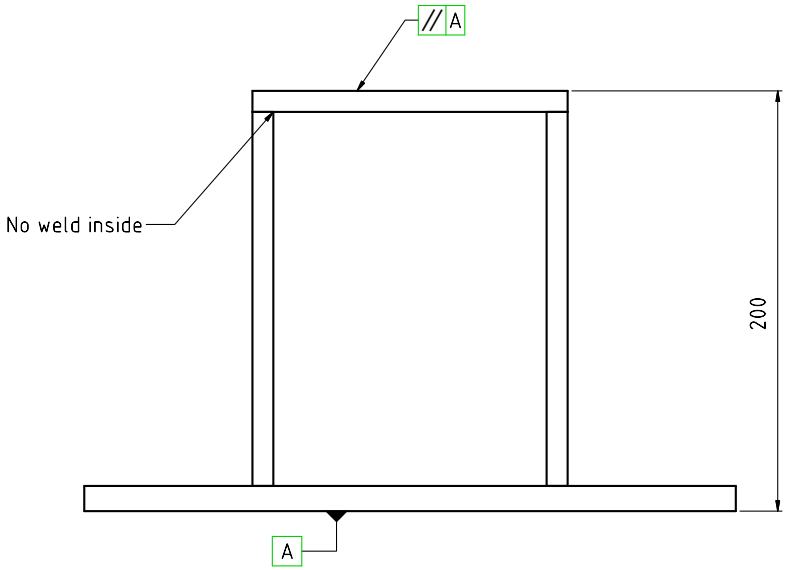

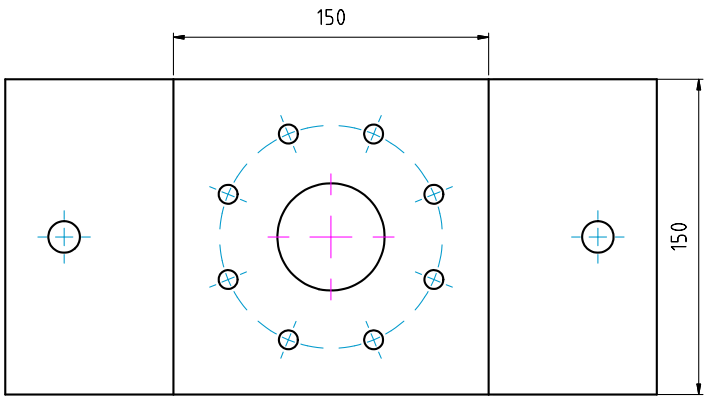

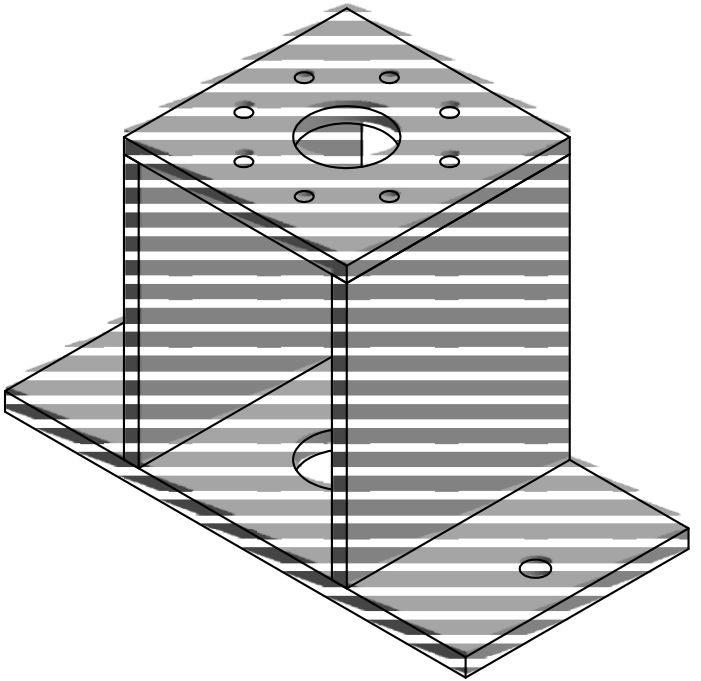

E 1:2

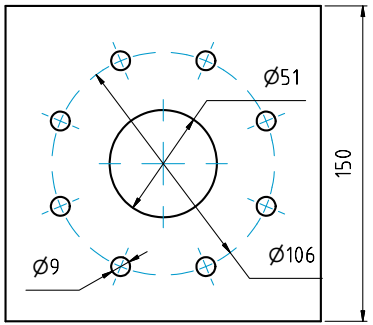

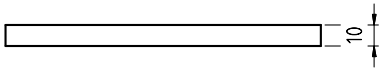

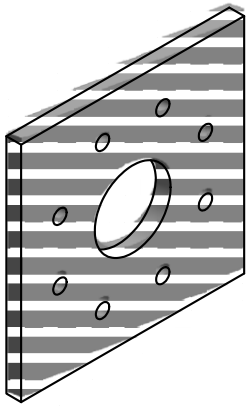

E 1:2

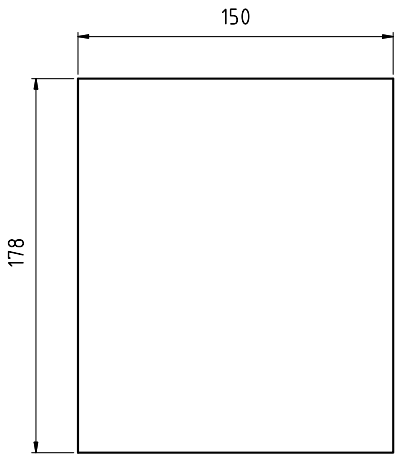

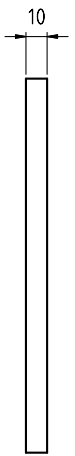

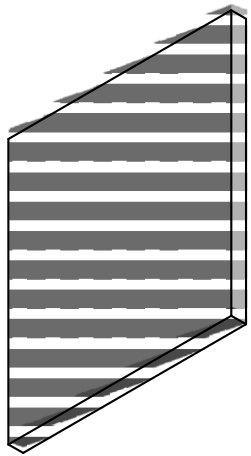

E 1:2

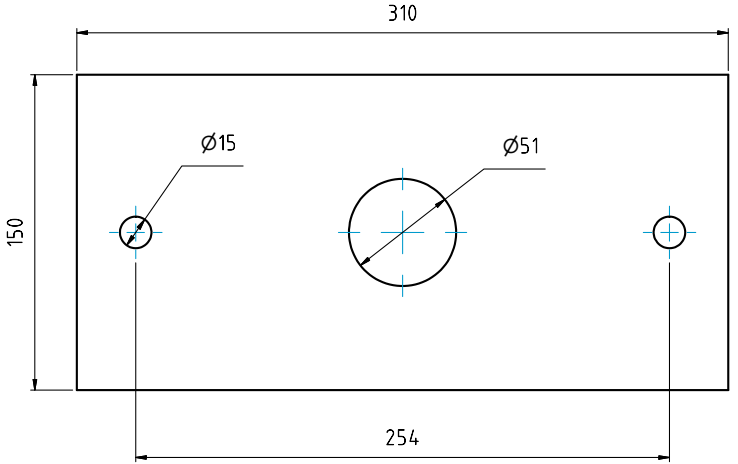

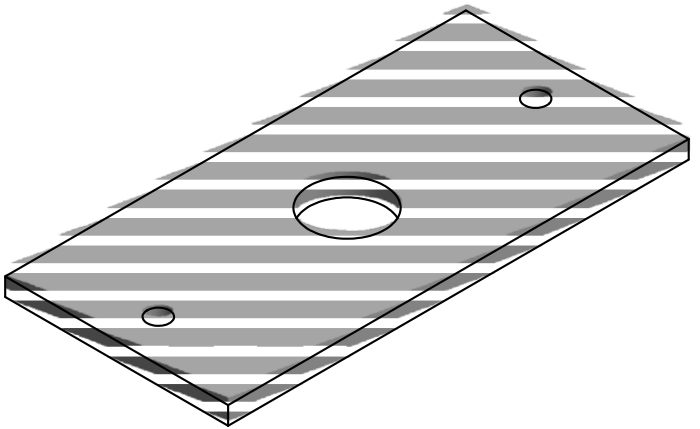

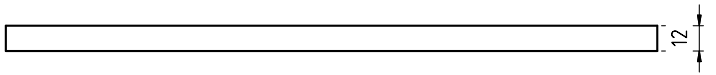

E 1:2

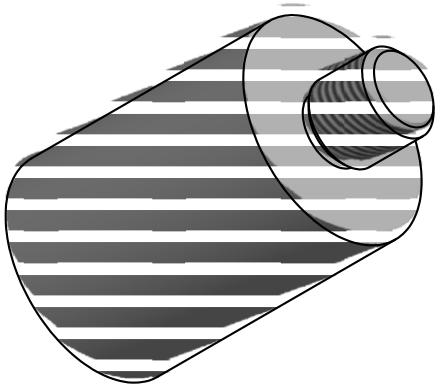

E 3:1

A-A (3 : 1)